PILOT-SCALE TEST OF WATER WASH CARBON DIOXIDE ABSORPTION SYSTEM FOR PURIFYING LANDFILL GAS AT JONES ISLAND WASTEWATER RECLAMATION FACILITY

by

Rebecca Schruender

A Thesis Submitted in

Partial Fulfillment of the

Requirements for the Degree of

Master of Science

in Engineering

at

The University of Wisconsin-Milwaukee

December 2019

ABSTRACT

PILOT-SCALE TEST OF WATER WASH CARBON DIOXIDE ABSORPTION SYSTEM FOR PURIFYING LANDFILL GAS AT JONES ISLAND WASTEWATER RECLAMATION FACILITY

by

Rebecca Schruender

The University of Wisconsin-Milwaukee, 2019
Under the Supervision of Professor Jin Li

Biogas, a product of the digestion of organic material, consists primarily of methane and carbon dioxide. By purifying raw biogas, or removing the carbon dioxide, it can be upgraded to biomethane, which can be used to generate heat and electricity or as a substitute for natural gas. An effective method of biogas purification is the water wash process, which consists of an absorption column in which a stream of biogas runs counter-current to a stream of water. The carbon dioxide dissolves in the water, increasing the methane concentration of the gas. A pilot scale system was operated at Jones Island Wastewater Reclamation Facility in Milwaukee Wisconsin to evaluate the effectiveness of this process by treating landfill gas. The effects of water flow, gas flow, and the gas/water ratio on the water wash system's efficiency were examined. The system operated best at low gas flow rates, while determining an ideal water flow rate or gas/water ratio proved difficult due to the low water supply pressure.

TABLE OF CONTENTS

LIST OF FIGURES

LIST OF TABLES

ACKNOWLEDGEMENTS

I would first like to thank my academic advisor, Dr. Jin Li of the Civil and Environmental Engineering Department at the University of Wisconsin-Milwaukee. Her guidance and recommendations have kept me on track and moving forward in what has easily been the biggest undertaking of my life thus far.

Special thanks also go out to Bryan Johnson of Energy Tech Innovations. His explanations and operation of the pilot system at Jones Island were invaluable to the completion of this paper, as were the many resources he shared with me.

I'd also like to thank Md Abul Bashar for his earlier work on this project modeling the prospective water wash system, as well as sharing his information and data with me.

Chapter 1: Introduction

Biogas

Biogas is produced through the process of anaerobic digestion, or the decomposition of organic material (Nock, Walker, & Heaven, 2014). This material may consist of manure, food waste, municipal waste, and wastewater, and it may be sourced from wastewater treatment plants, landfills, and anaerobic digestors, among other sources (Cozma, Wukovits, Mămăligă, Friedl, & Gavrilescu, 2014; Rasi, 2009). Biogas consists primarily of methane and carbon dioxide, followed by small amounts of hydrogen sulfide (Nock et al., 2014). Lesser amounts of oxygen, nitrogen, ammonia, halogenated compounds, and volatile organic compounds can also be included (Belaissaoui et al., 2016; Cozma et al., 2013; Rasi, 2009). Table 1 shows the typical makeup of biogas as reported by different sources.

Typical Biogas Makeup			
	Nock, et al. (2014)	**Energy Tech Innovations (2016)**	**Rasi (2009)**
Methane	55-65%	50-65%	45-70%
Carbon Dioxide	35-45%	35-40%	30-45%

Table 1: Components of biogas according to different sources

The exact composition of biogas and the amount of contaminants vary with different sources as well as the time of year (Cozma et al., 2014; Rasi, 2009). Table 2 shows how the source of biogas affects its composition.

Biogas Makeup by Source			
	Landfill	**Wastewater Treatment Plant Sewage Digester**	**Organic Waste Digester**
Methane	45-55%	55-65%	60-70%
Carbon Dioxide	30-40%	35-45%	30-40%
Nitrogen	5-15%	<1%	<1%
Other	Often contains halogenated compounds		

Table 2: Composition of biogas based on its source (Table based on information published by Rasi, 2009)

Biogas has several uses. It can be burned to produce heat and electricity in combined heat and power plants, injected into a natural gas pipeline after purification, and it can even be used within the chemical industry as feedstock (Belaissaoui et al., 2016; Cozma et al., 2013; Energy Tech Innovations, 2016). Biogas may also substitute compressed natural gas as a vehicle fuel (Cozma et al., 2013; Energy Tech Innovations, 2016; Nock, et al., 2014; Rasi, 2009). According to Rasi (2009), using purified biogas in lieu of compressed natural gas in vehicles releases less nitrogen oxide, hydrocarbons, and carbon monoxide than traditional vehicle engines. Rasi says that nitrogen oxide emissions of natural gas and biomethane vehicles can be as much as 60-85% less than those from diesel fuel vehicles. Furthermore, production of particulates may decrease by 60-80%, and carbon monoxide emissions by 10-70% (Rasi, 2009).

Biogas purification.

According to Tynell, Börjesson, & Persson (2007), raw biogas typically consists of 55-75% methane, plus carbon dioxide and hydrogen sulfide, although reported methane content varies from study to study. The carbon dioxide in raw biogas cannot be used to produce energy like methane, and so its presence decreases the energy potential of the gas (Cozma et al., 2013). For example, untreated biogas that consists of 65% methane has a caloric energy value of 6.5 kWh/m^3, while the caloric energy value of 95% methane gas is 9.5 kWh/m^3, which is comparable to that of diesel and petroleum (Sugiharto, Sutijan, & Hidayat, 2015). Therefore, it can be seen that purified biogas makes a much more efficient fuel than raw biogas due to its greater methane content. Furthermore, moisture in the gas, as well as contaminants like hydrogen sulfide can cause corrosion within the system (Sugiharto et al., 2015). These contaminants, along with the carbon dioxide, are typically removed during the process of biogas purification (Belaissaoui et al., 2016).

In order to substitute biogas for natural gas, the biogas must be purified to 95% methane or greater (Bortoluzzi, Gatti, Sogni, & Consonni, 2014; Nock et al., 2014; Sugiharto et al., 2015; Tynell et al., 2007). This is accomplished by removing CO_2 and other impurities, such as hydrogen sulfide, nitrogen, oxygen, and ammonia (Belaissaoui et al., 2016). The gas must also be dried during the purification process to remove moisture (Bortoluzzi, 2014; Tynell et al., 2007). Figure 1 shows the separation of the raw biogas in the purification process into biomethane and off-gas, or waste gas.

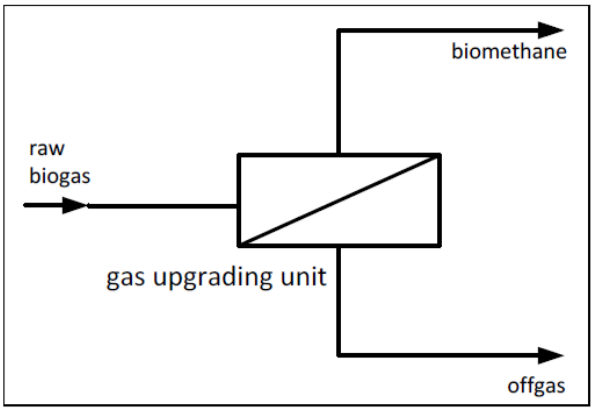

Fig. 1: Raw biogas is separated during the purification process into product gas (biomethane), consisting primarily of methane, and off-gas, which contains CO_2, H_2S, and other contaminants (Illustration credit: Sugiharto et al., 2015)

Methods of biogas purification.

Membrane separation.

Membrane separation is considered to be most applicable for small-scale plants, around 342Nm^3 biomethane/hr (Bortoluzzi et al., 2014). It is one of the most reliable and operable biogas purification systems, as it does not require any chemicals (Cozma et al., 2013). Membrane separation may also employ selective permeability to reduce methane loss. By using a dense skin membrane, less methane would be lost by dissolution in the solvent than in material-packed absorption columns (Belaissaoui et al., 2016). However, studies regarding the use of selective permeability have produced mixed results. Belsaissaoui et al. (2016) found that only membranes with a high selectivity produce significant results in improving biogas purity. At the same time, Cozma et al. (2013) report that other studies found membrane separation produces biogas with less purity than other upgrading methods.

Pressure-swing adsorption.

Pressure-swing adsorption operates on the principle that carbon dioxide molecules are smaller than methane. In this process, biogas flows past activated carbon, and carbon dioxide is retained in the pores of the carbon media. Methane molecules, on the other hand, are too large to fit in the pores, and continue to flow past the activated carbon, resulting in a product gas with a greater volume of methane. Pressure-swing adsorption is beneficial in that it is non-corrosive to equipment and it does not produce environmental pollutants as byproducts. On the other hand, it does have a high cost of operation and requires complex equipment. Additionally, the activated carbon media must regularly be desorbed of carbon dioxide (Sugiharto et al., 2015).

Absorption.

In this purification process, carbon dioxide is absorbed from the gas into a solvent, leaving methane in gaseous form. There are two primary types of solvent: physical solvents and chemical (Belaissaoui et al., 2016; Nock et al., 2014). When using a physical solvent, carbon dioxide transfers selectively from the gas to an aqueous phase. The solubility and partial pressures of the solutes determine equilibrium of the system (Bortoluzzi et al., 2014). An example of absorption with a physical solvent is pressurized water absorption, or PWA. PWA is one of the most efficient biogas purification processes (Belaissaoui et al., 2016). Chemical absorption, on the other hand, involves a chemical reaction, rather than dissolving the gas in the solvent. An aqueous alkanolamine solution, such as Mono Ethanol Amine, or Dimethyl Ethanol Amine, removes carbon dioxide from biogas by reacting with it (Bortoluzzi et al., 2014; Sugiharto et al., 2015). The amine solution reacts selectively with carbon dioxide, leaving the methane as a gas to be released (Sugiharto et al., 2015). When utilizing absorption processes for biogas purification, a balance must be maintained between obtaining biogas purity and

minimizing methane loss. Obtaining high purity of biogas usually results in greater methane slip, or the loss of methane in the biogas due to its dissolution in the solvent (Belaissaoui et al., 2016).

Absorption is an effective process which can achieve as high as 99% methane in product gas (Sugiharto et al., 2015). Additionally, carbon dioxide and hydrogen sulfide dissolve more easily in organic chemical solvents than in water, resulting in greater system efficiency (Rasi, 2009). Disadvantages of this method include the cost of the solvents and operations. Chemical solvents are more expensive than water, and large amounts of energy are required to regenerate the amine solvent in chemical absorption (Bortoluzzi et al., 2014; Rasi, 2009; Sugiharto et al., 2015). Amine-based absorption also requires more energy to regenerate the alkanolamine solution than physical absorption processes because the chemical bonds between the CO_2 and amine must be broken by supplying energy in the form of heat, which can require temperatures as high as 140-160^{o}C (Bortoluzzi et al., 2014). Finally, the solvent can also be corrosive and damage the system equipment (Sugiharto et al., 2015).

Water wash.

Water wash is an absorption-based biogas purification method. It is also called high-pressure water scrubbing or pressurized water absorption (Belaissaoui, et al., 2016; Cozma et al., 2013). The water wash method uses pressurized water as a solvent to remove carbon dioxide from biogas and is considered to be best for large-scale (753Nm^3 biomethane/hr) biogas purification operations (Bortoluzzi, et al., 2014; Sugiharto et al., 2015; Tynell et al., 2007). It is one of the most common gas purification methods and also tends to have a lower cost than others. Multiple studies have found that water wash is “one of the simplest and most economical methods” of biogas purification. It is important to note, however, that the incorporation of a water regeneration system increases energy usage and costs. Additional benefits include the system’s good reliability, and easy maintenance, as well as its ability to remove carbon dioxide and hydrogen sulfide together. At low hydrogen sulfide concentrations,

pretreatment of the gas before entering the water wash system is not necessary (Cozma et al., 2014). Otherwise, at high levels, H_2S should be removed before the gas enters the absorbers if the water is to be recycled, to prevent potential fouling issues (Nock et al., 2014).

In the water wash process, raw gas is first dewatered in a separator, where condensation is used to remove the water. The gas is then pressurized to 9-12 bar in a compressor to increase carbon dioxide solubility and afterwards cooled in a heat exchanger (Bortoluzzi et al., 2014; Tynell et al., 2007). Since gas compression is accompanied by an increase in temperature, it must be cooled before entering the absorption column (Cozma et al., 2013). This promotes the dissolution of CO_2 to carbonic acid (H_2CO_3), as carbon dioxide dissolves to form carbonic acid better at low temperatures (Dodds, Stutzman, & Sollami, 1956; Tynell et al., 2007). Figure 2 shows the variation of carbon dioxide solubility at different pressures and temperatures.

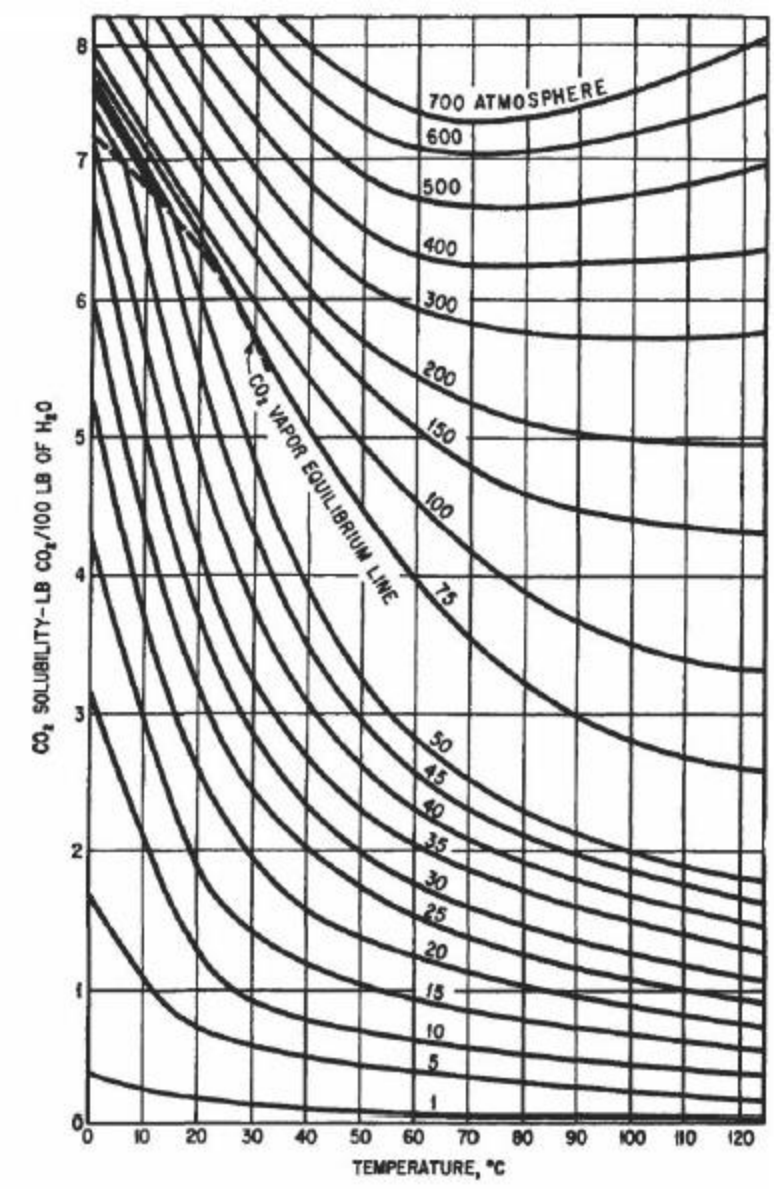

Fig. 2: The solubility of carbon dioxide in water increases with greater pressure and lower temperature (Illustration credit: Dodds et al., 1956)

After compression and cooling, the gas then enters the absorption column, a tall, narrow cylinder, which is often roughly 10m high and 0.5m in diameter. Water is fed into the column from the top, and gas, still pressurized, enters from the bottom so that they run counter-current to each other. Inside, the column is filled with packing material to increase the contact area between the water and the

gas (Tynell et al., 2007). Greater contact area between the water and gas results in greater mass transfer efficiency. To further increase contact area, gas is either dispersed in small bubbles into a continuous liquid stream, or liquid is dispersed as small droplets or spread in a thin film into a continuous gas stream (Rasi, 2009). The packing material consists of pall rings, which are plastic cylindrical rings typically 25mm in height and 25mm in diameter. When the water and gas come into contact with each other as the water flows over the pall rings, the carbon dioxide in the raw biogas dissolves into the water, forming carbonic acid (Tynell et al., 2007). The methane remains in gas form, as it dissolves less readily in water than carbon dioxide (Nock et al., 2014)--Carbon dioxide is approximately 25-26 times more soluble in water at 25^{o}C than methane (Bortoluzzi et al., 2014; Energy Tech Innovations, 2016). Likewise, nitrogen and oxygen are less soluble in water than carbon dioxide and hydrogen sulfide. Lesser amounts of these constituents, which may also be present in raw biogas, remain mixed with the methane gas (Cozma et al., 2014).

This relationship can also be described by Henry's Law. The partial pressure of a gas is directly related to its concentration in solution in a liquid/gas system, as given by Equation 1 (*Carbon Dioxide,* 2018; Rasi, 2009).

$$P_A = K_A X_A \qquad \text{Equation 1}$$

Where: P_A is the partial vapor pressure of gas A (bar)

K_A is Henry's Law constant for gas A (mol/kg*bar)

X_A is the mole fraction gas A in aqueous solution (mole gas/mole solution)

Henry's Law constant for methane is reported to be between 0.0013 and 0.0015 mol/kg*bar (*Methane*, 2018). For carbon dioxide, it is 0.031-0.035 mol/kg*bar, and hydrogen sulfide has a Henry's Law constant of 0.097-.1 mol/kg*bar (*Carbon Dioxide*, 2018; *Hydrogen Sulfide,* 2018). Because the Henry's Law constant for methane is significantly lower than those for carbon dioxide and hydrogen sulfide, the majority of methane remains in the gaseous phase while carbon dioxide and hydrogen sulfide dissolve in the water of the absorption column. The methane gas continues to rise, leaving the column from the top (Rasi, 2009). This purified biogas consists of 95% or greater methane (Nock et al., 2014).

While in the absorption column, small amounts of methane dissolve in the solvent along with the carbon dioxide and hydrogen sulfide. To decrease this methane slip, or loss of methane to the purification process, the water enters a flash tank after leaving the absorption column to remove this methane. In the flash tank, the pressure is decreased to an intermediate pressure of 2-4 bars, releasing the methane from the water (Rasi, 2009; Tynell et al., 2007). While most of the carbon dioxide remains dissolved in the water at this pressure, most of the dissolved methane is released because of its lower Henry's Law constant—The lower the constant value, the more volatile a substance is. Carbon dioxide is less volatile than methane, and therefore, the majority of it remains dissolved in the process water, even in the reduced pressure of the flash tank. The released gas is then returned to the raw biogas stream ahead of the compressor and reenters the absorption column (Bortoluzzi et al., 2014; Tynell et al., 2007). Without the benefit of a flash tank, methane dissolved in the absorber column may be released to the atmosphere with other waste gas (Rasi, 2009). Nock et al. (2014) found that without a flash column, methane losses can be as high as 6% at 10 bar, and as high as 12% at 20 bar. In addition to the loss of this methane as potential fuel, it is also a greenhouse gas. Methane is 23 times more potent as a greenhouse gas than carbon dioxide, making its recovery even more important (Sugiharto et al.,

2015). However, including a flash tank in the system can reduce methane loss to less than 1% (Nock et al., 2014).

From the flash tank, the water may be regenerated in a desorption column, or CO_2 stripper (Bortoluzzi et al., 2014; Tynell et al., 2007). Regeneration is typically used when the process water is of drinking water quality. This process acts as a cost-saving measure by minimizing the need for a continuous stream of treated drinking-quality water. In this column, carbon dioxide is removed from the process water so the water can be recycled to the absorption column to purify additional biogas. The desorption column contains pall rings like the absorption column, and the water also similarly enters the desorption column from above, while inert gas is pumped in from below. The gas displaces the carbon dioxide dissolved in the process water, thereby increasing the pH through the CO_2 removal, and regenerating the water for reuse in the absorption column. The temperature of the water increases during the stripping process, so a heat exchanger it utilized to cool it to approximately 15^{o}C, which is a commonly used temperature for CO_2 absorption (Tynell et al., 2007). After the stripping process is complete, the process water is recirculated back to the absorption column to repeat the cycle (Bortoluzzi et al., 2014). Regenerating process water for reuse can be cost effective in situations where a constant supply of water is not readily available, as it may use almost 100 times less water than non-regenerating systems (Cozma et al., 2014).

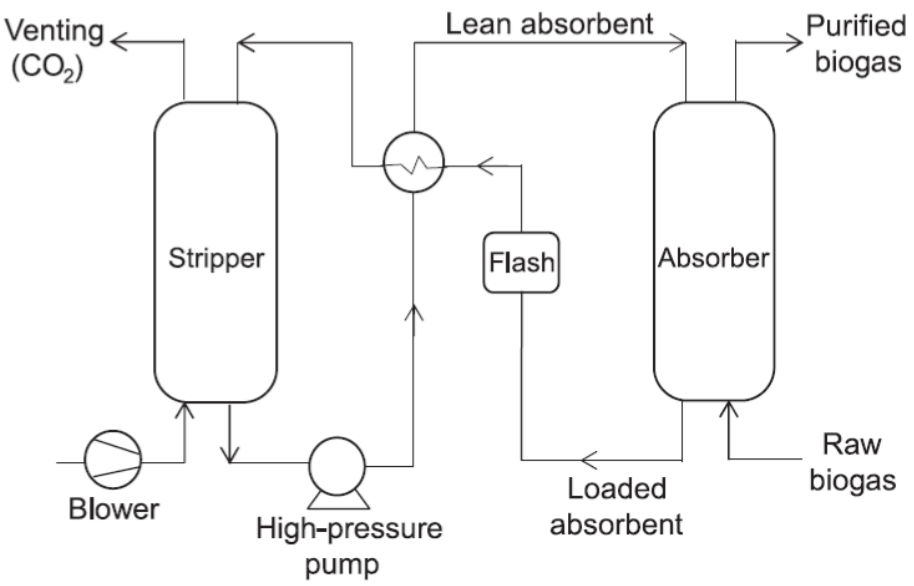

Fig. 3: Diagram of a biogas purification system with process water regeneration for continuous reuse (Illustration credit: Belaissaoui et al., 2016)

As an alternative cost-saving measure, treated wastewater may be used for the CO_2 absorption process, rather than potable water. In this scenario, the water wash is set up as a single-pass system, in which the process water is not regenerated and only flows through the absorption column one time. As in the water regeneration model, the water removes CO_2 from raw biogas in the absorption column, and undergoes depressurization to release dissolved methane in the flash tank. However, after leaving the flash tank, the water, still containing the dissolved carbon dioxide, returns to the wastewater treatment plant processes. This has the advantage of reducing water supply costs, as the plant has a continuous source of low-cost water supply. There is, however, much more variation in water temperature from season to season than water used in a regenerative water wash process. Water temperatures can vary as much as 20^{o}C or more (Tynell et al., 2007). This would likely affect the efficiency of the water wash system, as carbon dioxide dissolves in water more readily at low temperatures than high, as shown in Figure 2 on page 8 (Dodds et al., 1956; Tynell et al., 2007).

Benefits of water wash purification.

There are several advantages to the water wash method of biogas purification. Energy produced from the product gas can be used to power the purification process. It has been reported that the energy consumption of water regeneration plants was equal to only 3-6% of the energy content of the purified gas, while other studies found that as much as 11% of the biomethane's energy content was required to upgrade the raw biogas. However, it is unknown which method was used to upgrade the gas in this case (Nock et al., 2014). Cozma et al. (2013) calculated in an Aspen Plus software simulation that the purification process requires approximately 5.7% of the upgraded biomethane's energy content. This makes it one of the most cost-efficient biogas purification processes (Cozma et al., 2014; Sugiharto et al., 2015). Additionally, no chemicals are required, as pressurized water is the only acting absorbent. Finally, water wash also has the lowest unit cost for biogas upgrading (0.15 €/Nm^3), with high purity results (up to 98% methane) (Cozma et al., 2013). Sugiharto et al. (2015) found similar results when comparing water scrubbing, pressure swing adsorption, chemical scrubbing, membrane separation, and cryogenic upgrading, as shown in Table 3.

	Water Scrubbing	PSA	Chemical Scrubbing	Membrane Separation	Cryogenic
Investment Cost (€/year)	€ 265, 000	€ 680, 000	€ 353, 000 - 179, 500	€233, 000 - 749, 000	€ 908, 500
Maintenance Cost (€/year)	€ 100, 000	€187, 250	€134, 000 - 179, 500	€ 81, 750 - 126, 000	€ 397, 500
Cost per Nm^3/biogas upgraded	0.13 €	0.25 €	0.17 - 0.28 €	0.12 - 0.22 €	0.44 €

Table 3: Cost of different biogas purification methods Source credit: Sugiharto et al., 2015

Disadvantages of water wash purification.

Disadvantages of the water wash purification process include the possibility of microbial growth, and release of greenhouse gases. Tynell et al. (2007) found that single pass systems may be more likely to experience microbial growth on the column packing material, which affects process efficiency, due to the lower water quality. Additionally, if hydrogen sulfide is present in high concentrations, H_2S dissolved in process water must be removed before entering the desorption column in water-regeneration systems. Hydrogen sulfide reacts with the air dispersed into the system in the desorption column to form H_2SO_4, which is corrosive. If corrosion is a possibility, H_2S may be removed with a pre-treatment step before gas enters the absorption column (Nock et al., 2014). The possibility of a high pressure drop across the column and flooding of the column are other disadvantages (Cozma et al., 2014). Finally, emissions of carbon dioxide, hydrogen sulfide and other contaminants removed from biogas must be minimized. Carbon dioxide is a greenhouse gas, and hydrogen sulfide is toxic at concentrations greater than 10ppm and has corrosive properties, so both should be contained rather than released to the atmosphere if large quantities are produced (Cozma, et al., 2013).

Aspen Plus Simulation Software

Aspen Plus Simulation Software can model dissolution of gases in water using multiple thermodynamic models. These models are UNIQUAC (with ideal gas and Henry's Law), NRTL (non-random-two-liquid with idea gas and Henry's Law), NRTL-RK (non-random-two liquid/Redlich-Kwong equation of state with Henry's Law), UNIQ-RK (UNIQUAC/Redlich-Kwong equation of state with Henry's Law), and ELECNRTL (electrolytic non-random two liquid model with Redlich-Kwong equation of state for aqueous and mixed solvent applications with Henry's Law) (Cozma et al., 2014). The software includes pre-defined equipment, including heat exchangers, pumps, reactors, and compressors, and can model

operations of an entire plant using the thermodynamic models, material properties, and unit operation models (Cozma et al., 2013).

Chapter 2: Materials and Methods

Water Wash Gas Purification

As a substitute for biogas, this project purified landfill gas which was piped to Jones Island Water Reclamation Facility in Milwaukee, WI. The water wash purification method was selected for its low cost and reasonable product gas purity. Two carbon dioxide absorption columns were designed by Energy Tech Innovations at a pilot scale size. In this setup, the landfill gas flows upwards from the bottom of the column, counter-current to a water stream which flows down the column. The water used in this experiment was treated city water, at a steady temperature of approximately 50^{o} F. The purified product gas, consisting primarily of methane, is collected at the top of the column, while the carbon dioxide-rich process water exits the absorption column to enter the flash column.

The flash columns, like the absorption columns, were designed by ETI for this pilot-scale project. The flash columns operate at a lower pressure than the absorption columns, allowing some of the dissolved gas (specifically, any dissolved methane) to be released from the aqueous phase. Because this released gas contains some carbon dioxide in addition to the recollected methane, it is directed back to the beginning of the process flow to reenter the absorption column with the landfill gas stream. Figure 4 provides a diagram of the pilot system setup. The return of slip gas from the flash column is not depicted in this figure.

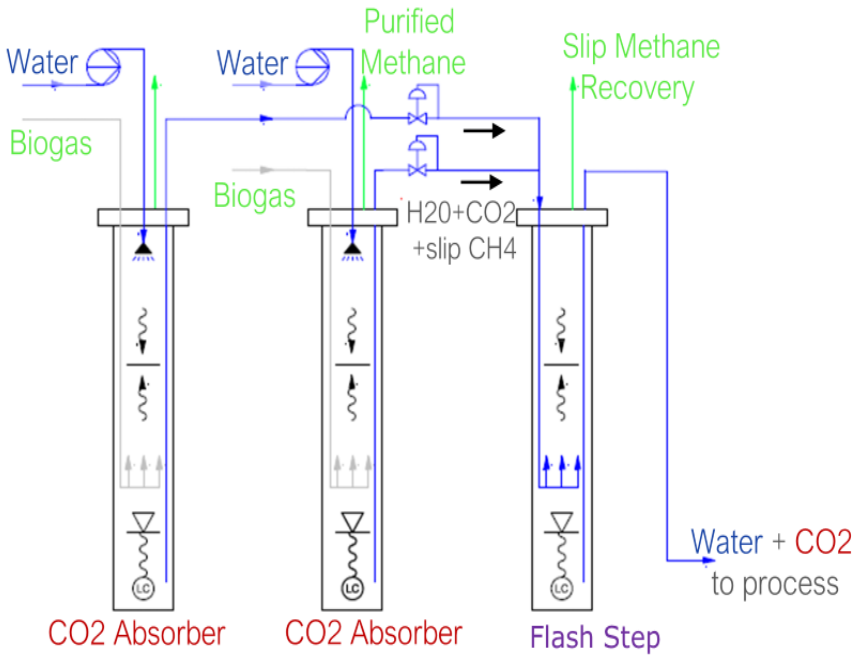

Fig. 4: Diagram of water wash process including carbon dioxide absorption columns and flash column (Illustration courtesy of Energy Tech Innovations)

The methane, carbon dioxide, nitrogen, and oxygen content of the biogas was measured both before and after purification using a Landtec GEM 2000 landfill gas meter. Independent variables in these experiments included the rate of gas flow, rate of water flow, and the gas:water flow rate ratio. Due to low water pressure and water flow, operation was limited to one absorption column, with no flash process.

Chapter 3: Results

Biogas Purification Results

The efficiency of CO_2 removal was evaluated by calculating the performance index, ξ, as given by Nock et al. (2014) Equation 2 is used to calculate ξ:

$$\xi = \frac{1-y_e/y_r}{1-y_e/100} \qquad \text{Equation 2}$$

Where: y_e=Mole fraction of CO_2 in enriched biogas

y_r=Mole fraction of CO_2 in raw biogas

When calculating the performance index, the measured percentage of carbon dioxide in the raw and purified landfill gas was used as the mole fraction of carbon dioxide. The assumption was made that only carbon dioxide, methane, oxygen, and nitrogen were present in the unpurified gas, and that it contained no additional unmeasured gases. The effect on performance index of water flow, gas flow, and water/gas ratio is shown in Figures 5-7. Figure 5 shows no correlation between water flow rate and performance index, while Figure 6 would indicate a fairly strong negative correlation between landfill gas flow rate and the performance index. Figure 7, meanwhile, shows a more moderate negative relationship between gas/water ratio and performance index. It should be noted that the data shown in these graphs was not controlled for all variables. The three variables evaluated are water flow rate, gas flow rate, and gas:water ratio. However, all three of these variables changed from run to run, which was often necessary to keep the absorption column in balance so that it did not flood or become under-

pressurized. Figures 5-15 show the full dataset without consideration for how the variables were controlled. Control of additional variables aside from the independent variable is discussed later in this section.

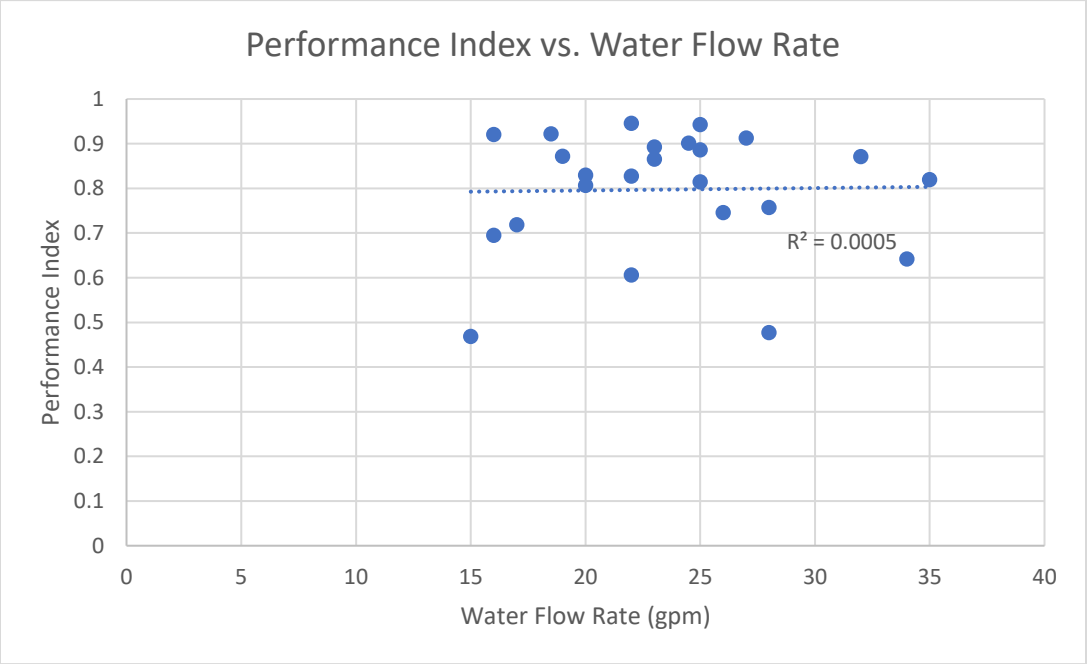

Fig. 5: Performance index versus water flow rate

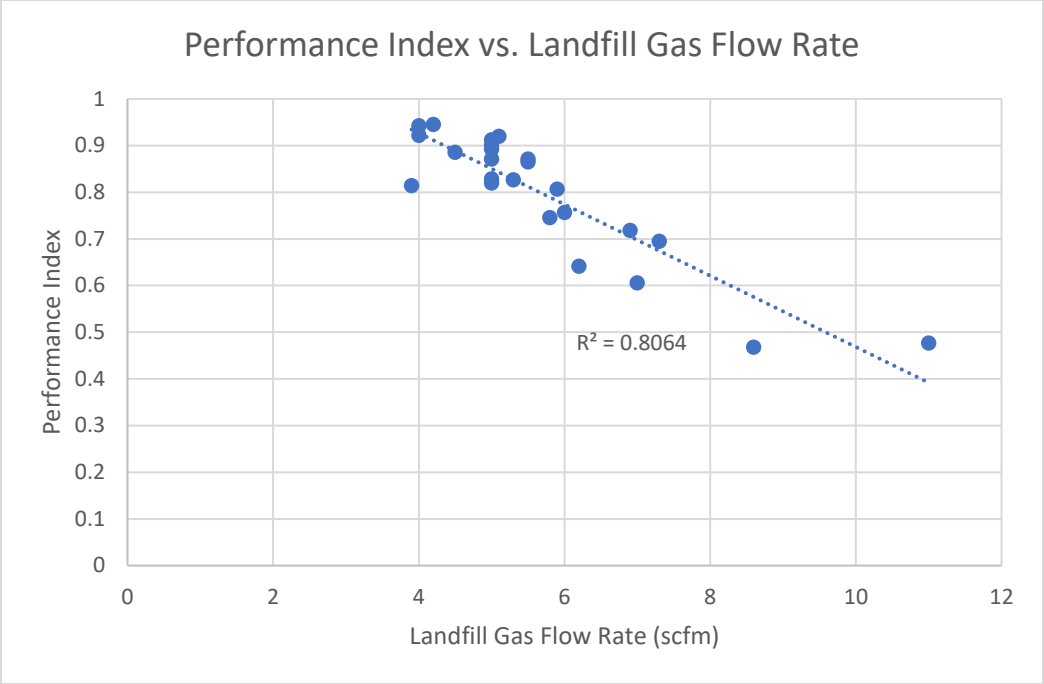

Fig. 6: Performance index versus landfill gas flow rate

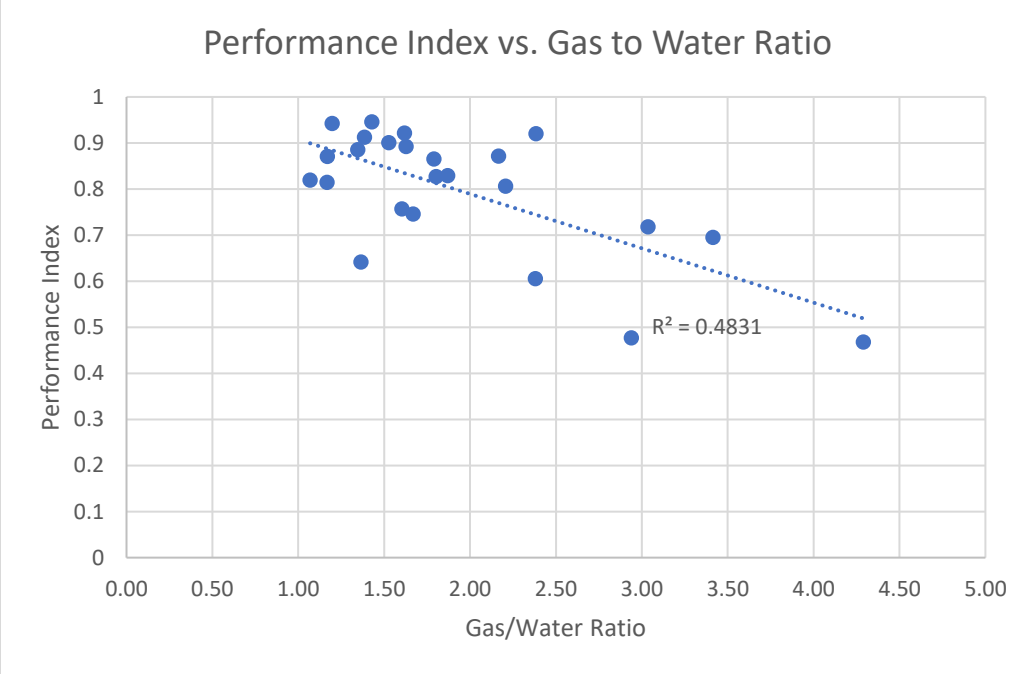

Fig. 7: Performance index versus water/gas ratio

Figures 8 and 9 show the relationship between performance index and percent change in methane and carbon dioxide content, respectively, from the raw gas to the product gas. They both demonstrate a strong correlation between increasing performance index values and increasing methane content/decreasing carbon dioxide content.

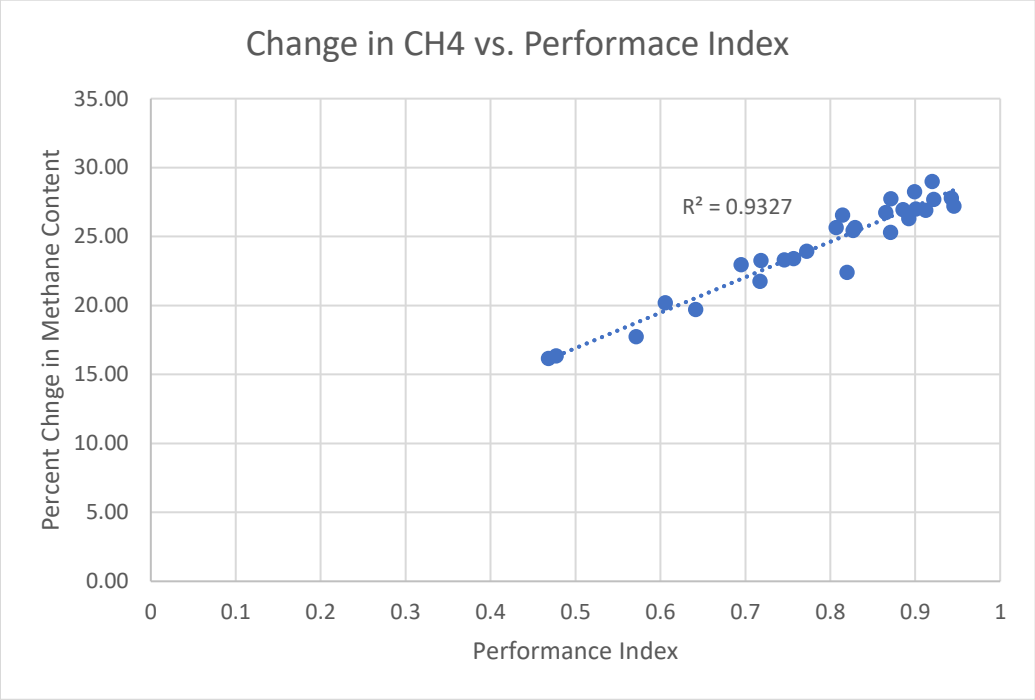

Fig. 8: Change in methane content of landfill gas versus performance index

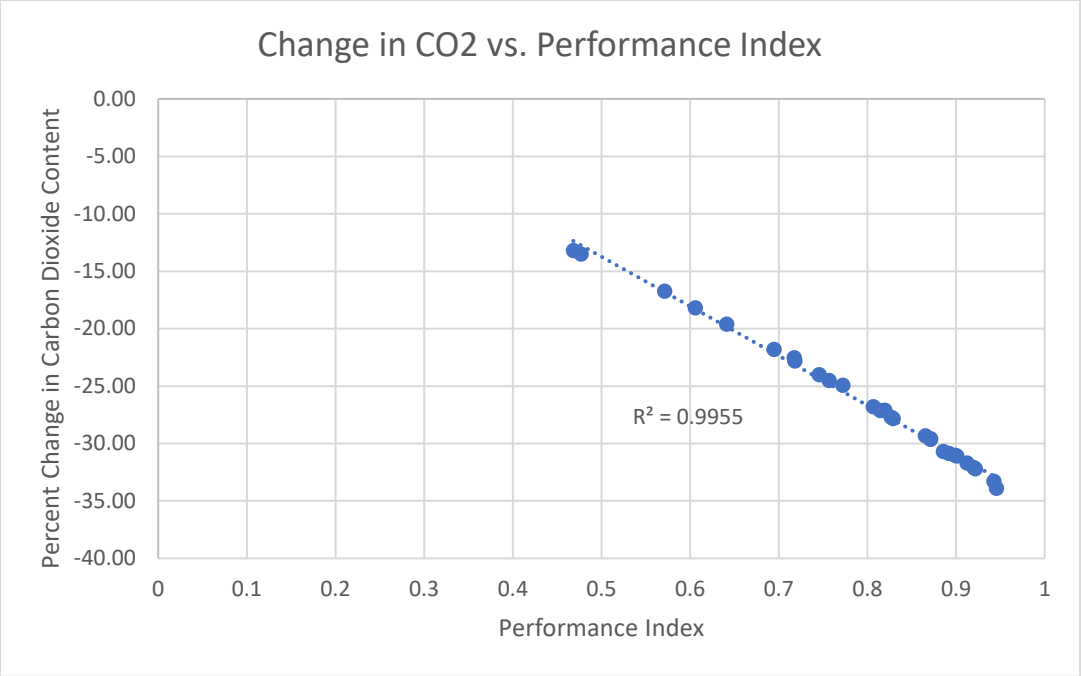

Fig. 9: Change in carbon dioxide content versus performance index

Figures 10 and 11 focus on the relationship between water flow rate and change in methane and carbon dioxide contents of the gas. No correlation is apparent from the datapoints shown in these figures.

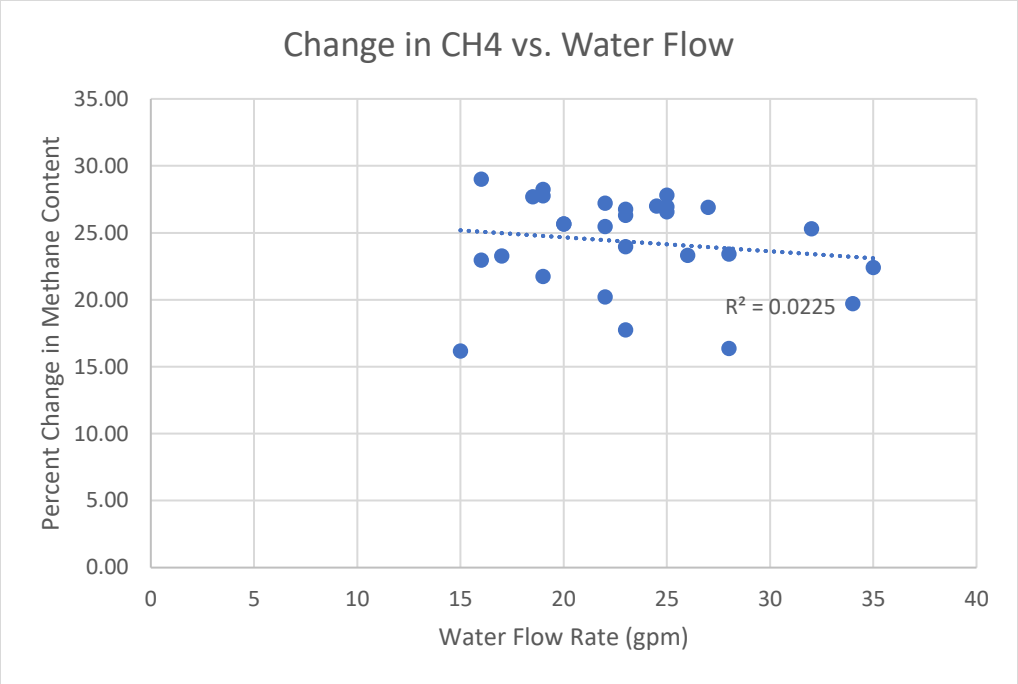

Fig. 10: Percent change in methane content versus water flow rate

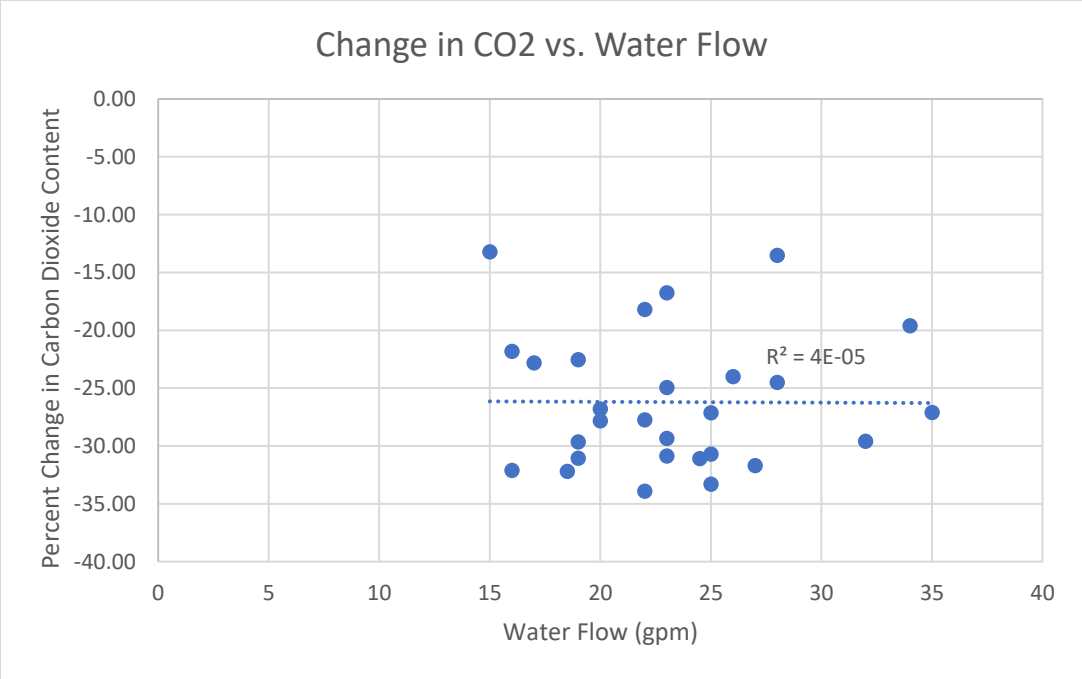

Fig. 11: Percent change in carbon dioxide content versus water flow rate

A moderate correlation was observed between changes in landfill gas content and landfill gas flow rate. Increases in gas flow rates were associated with less change in methane content and lower rates of carbon dioxide absorption, as shown in Figures 12 and 13, below.

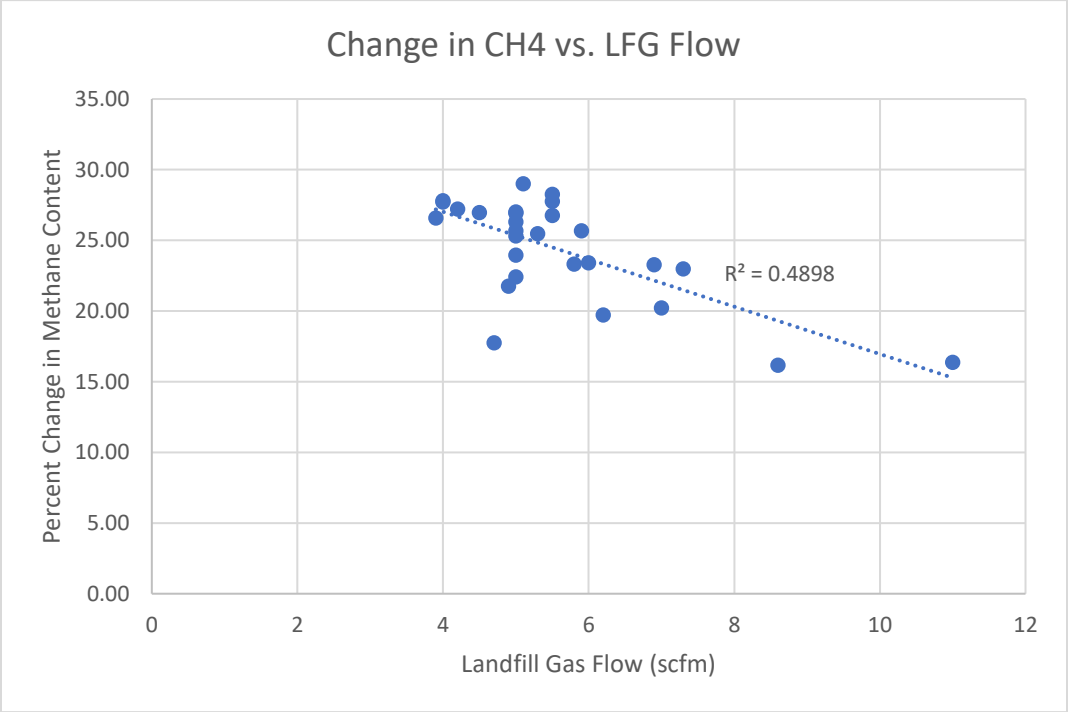

Fig. 12: Percent change in methane content versus landfill gas flow rate

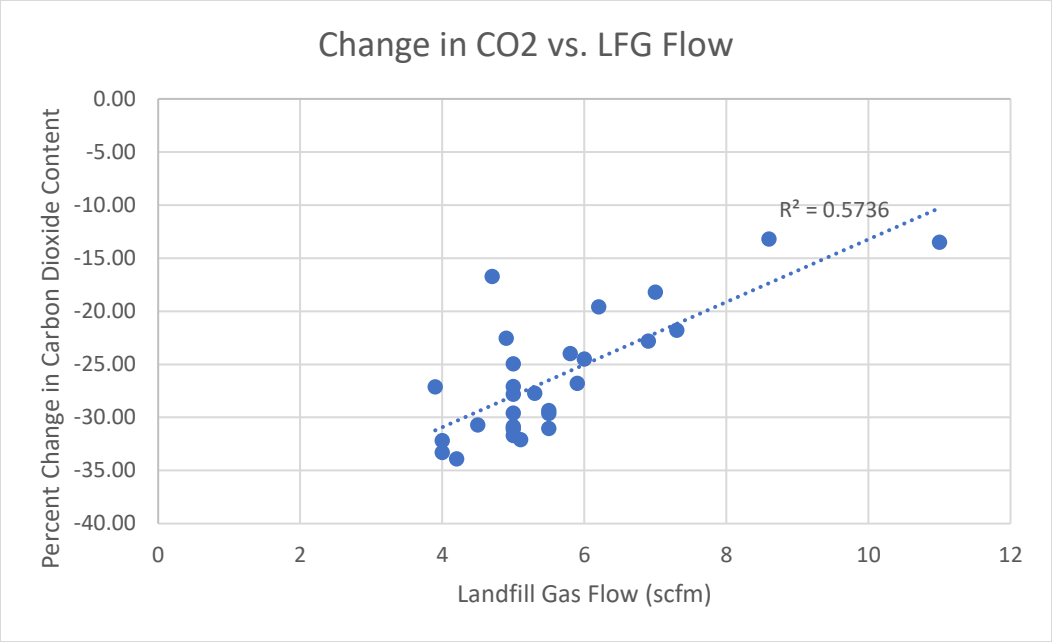

Fig. 13: Percent change in carbon dioxide content versus landfill gas flow rate

The effect of gas/water ratio on changes in methane and carbon dioxide content is shown in Figures 14 and 15. These figures indicate decreases in percent change of both methane and carbon dioxide with greater gas/water ratios; however, the correlation is poor; low R^2 values for both graphs indicate a poor fit to the regression line.

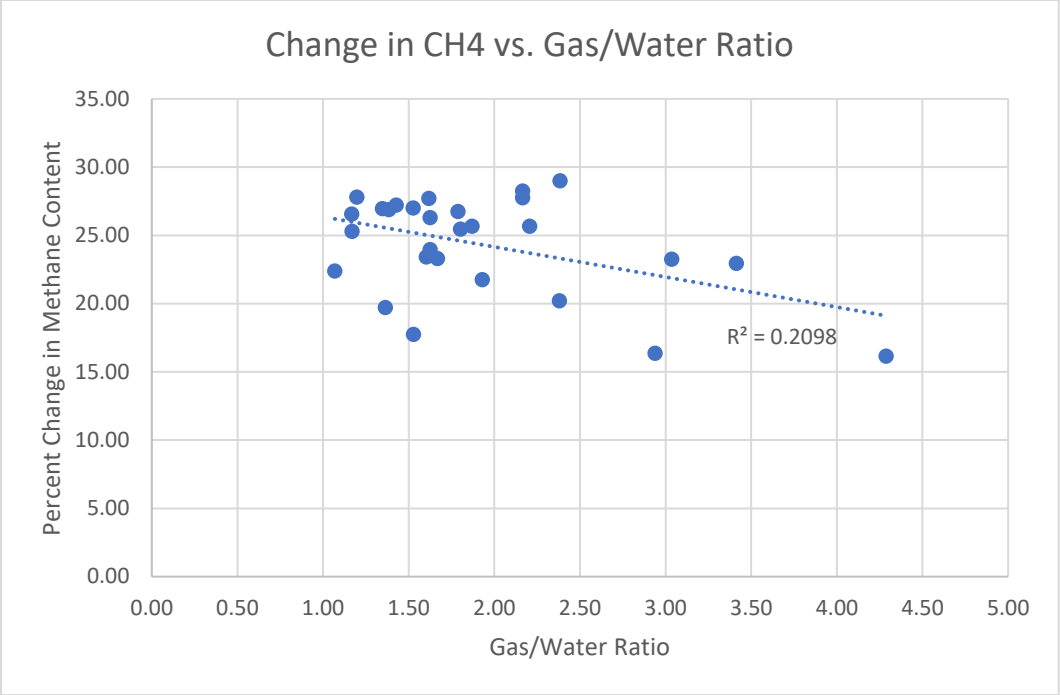

Fig. 14: Percent change in methane content versus gas/water ratio

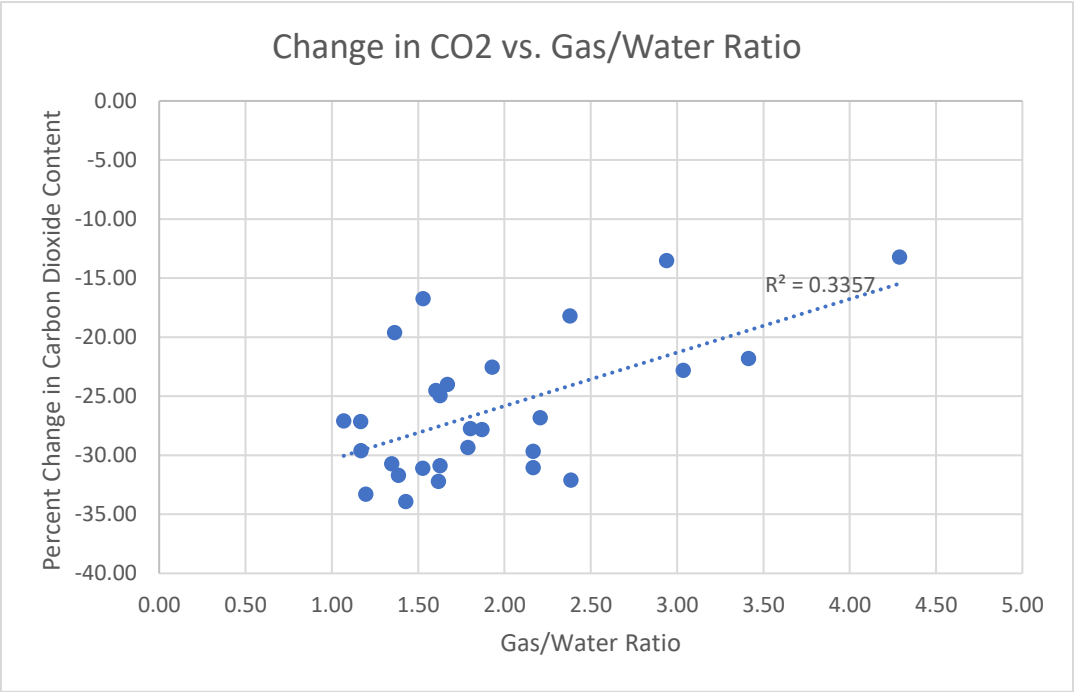

Fig. 15: Percent change in carbon dioxide content versus gas/water ratio

Controlling for multiple variables.

Methane and carbon dioxide contents of the product gas were analyzed based on the input flow rates of water and landfill gas and the gas/water ratio. As mentioned above, multiple variables changed between runs when evaluating an independent variable during this experiment. To account for this, data points were afterwards separated and grouped based on two of the three possible control variables. First, the measured values of landfill gas flow, water flow, and gas/water ratio for each data point were separated into groups of similar values. The range of each group was selected so that each cluster consisted of four to thirteen data points, although groups of one to two outliers were also present. Table 4 shows the range of each grouping. By grouping the data set based on similar values, these variables are controlled so the relationship between one of the variables and change in landfill gas content can be isolated. This allowed the changes in methane and carbon dioxide content of the gas to be plotted against a control variable such as the gas/water ratio for these points while controlling for both of the other control variables—In this case, the water and gas flow rates. As an example, the effect of gas/water ratio on methane content is evaluated for moderate landfill gas flows and high water flows in Figure 16. Figure 17 likewise shows the change in methane content with gas/water ratio at low to moderate gas and water flows. The same analysis is applied to change in carbon dioxide content of the landfill gas during the purification process, as shown in Figures 18 and 19.

Gas/Water Ratio	Landfill Gas Flow (scfm)	Water Flow (gpm)
1.0-1.5	3.5-4.4	14-18
1.5-2.0	4.5-5.4	19-23
2.0-3.0	5.5-6.4	24-28
3.0-4.0	6.5-9.0	29-33
≥4	≥9	≥34

Table 4: Ranges of values for each data point grouping for gas/water ratio, landfill gas flow, and water flow

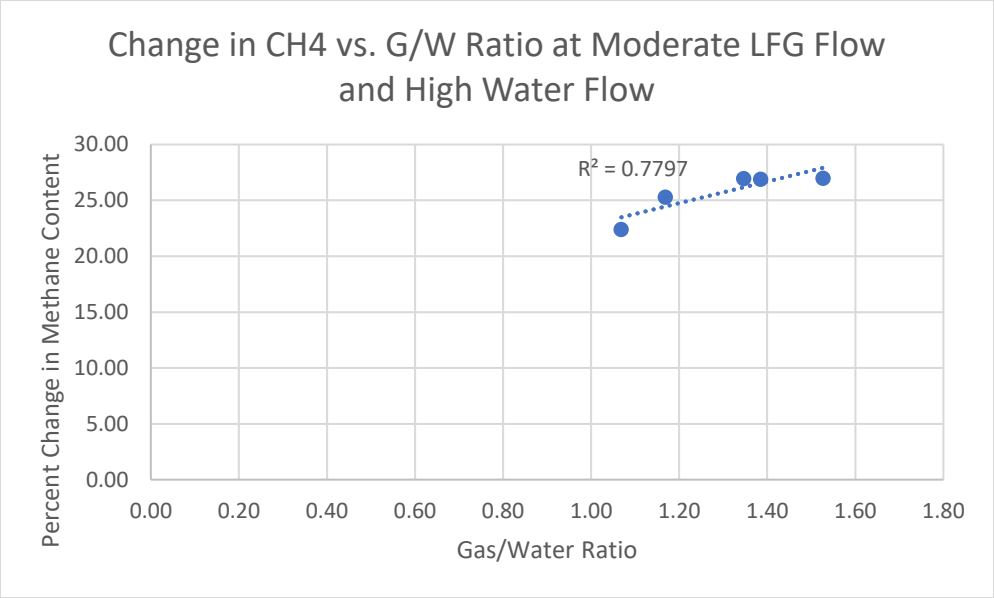

Fig. 16: The change in landfill gas methane content versus gas/water flow ratio at moderate landfill gas flow rates and high water flow rates

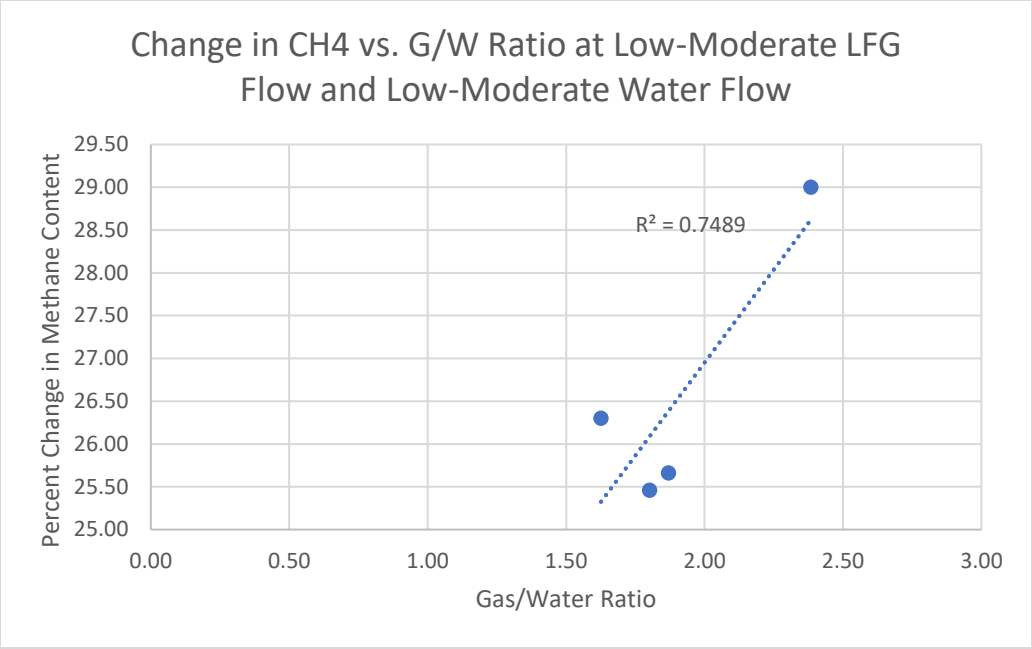

Fig. 17: The change in landfill gas methane content versus gas/water flow ratio at low-moderate gas and water flow rates

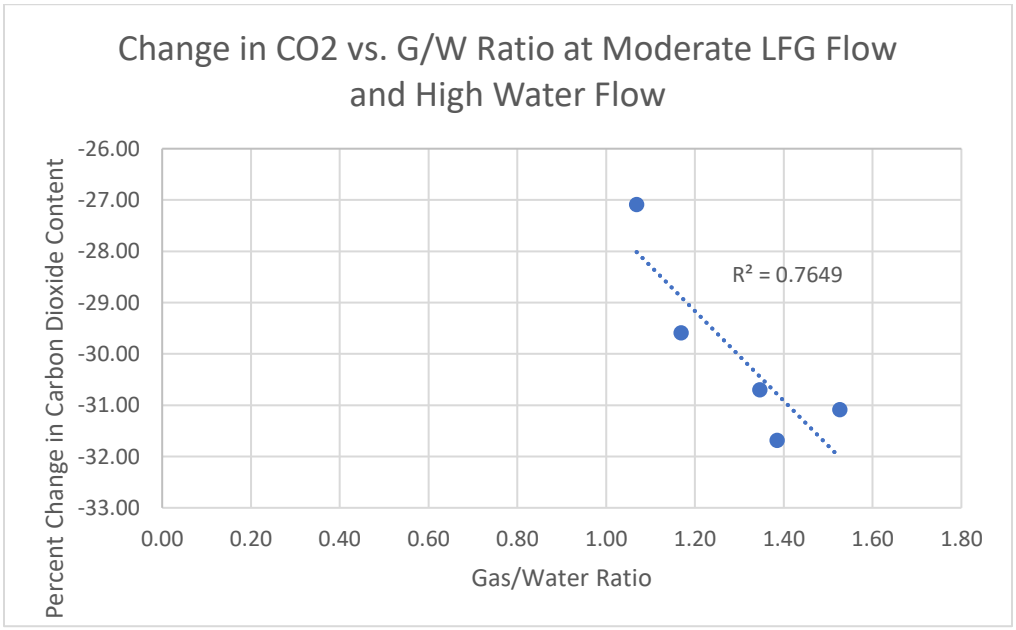

Fig. 18: The change in landfill gas carbon dioxide content versus gas/water flow ratio at moderate landfill gas flow rates and high process water flow rates

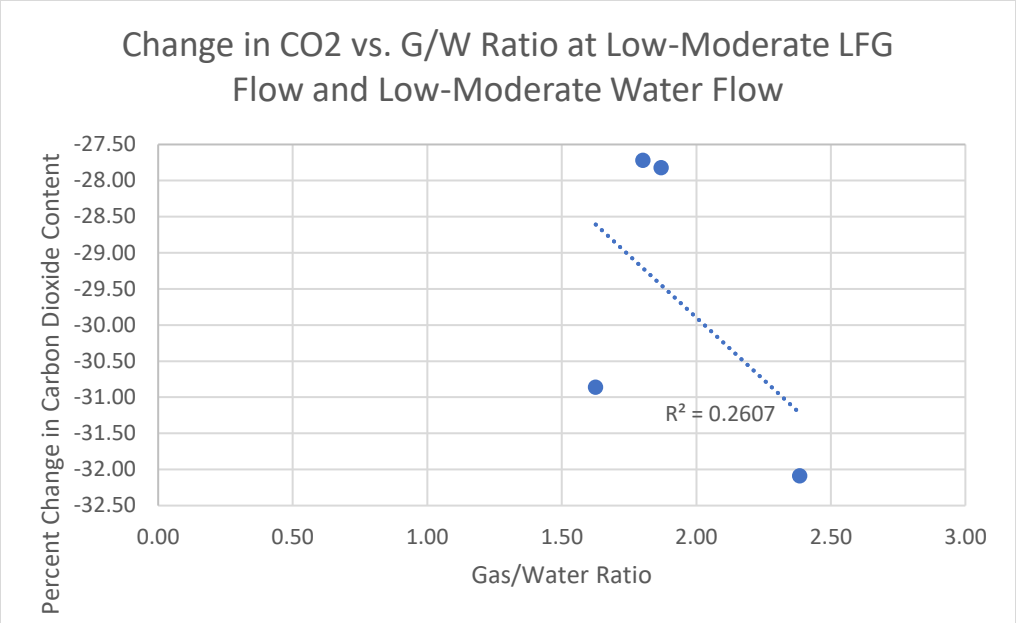

Fig. 19: The change in landfill gas carbon dioxide content versus gas/water flow ratio as low-moderate gas and water flow rates

Finally, the change in methane and carbon dioxide content with water flow rate at given landfill gas flow rates and gas/water ratios is shown in Figures 20 and 21, and Figures 22 and 23 show similar graphs with landfill gas flow rate as the dependent variable. The same process was followed to group data points with similar gas/water ratios to evaluate the specific relationships between gas or water flow rate and product gas content.

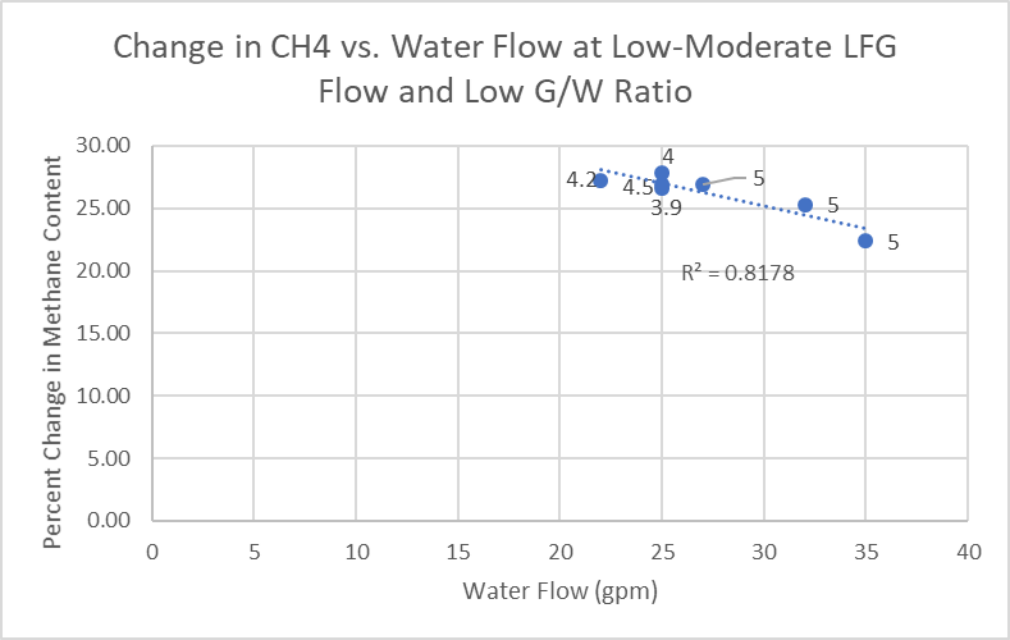

Fig. 20: The change in landfill gas methane content versus water flow rate at low-moderate landfill gas flow rates and low gas/water ratios—Data labels indicate landfill gas flow (scfm)

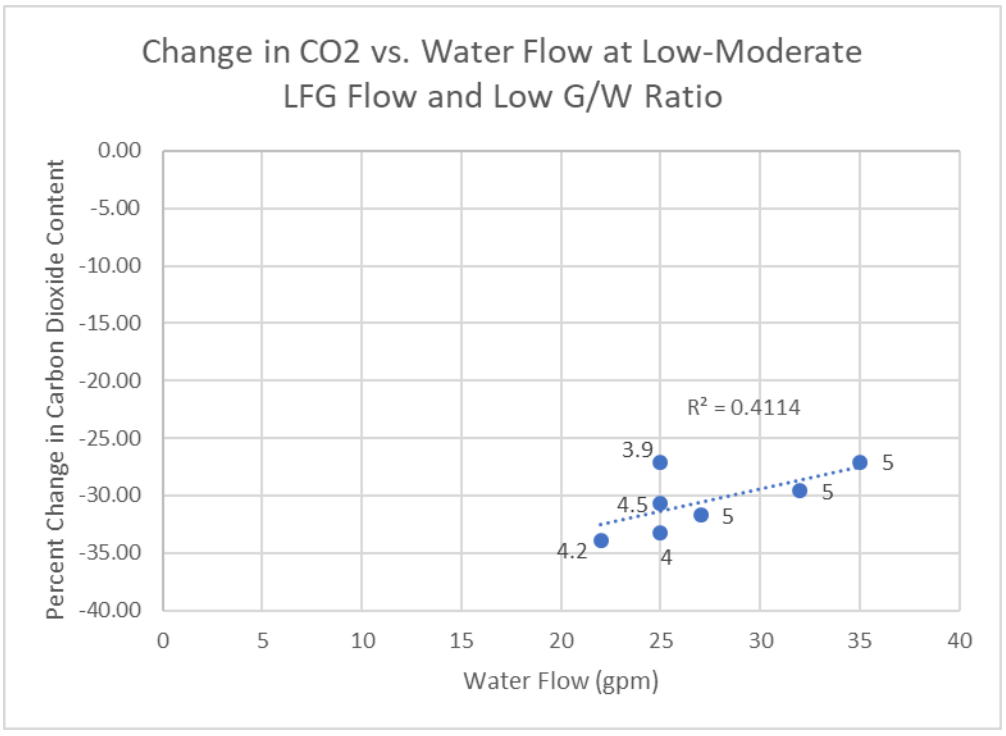

Fig. 21: The change in landfill gas carbon dioxide content versus water flow rate at low-moderate landfill gas flow rates and low gas/water ratios—Data labels indicate landfill gas flow (scfm)

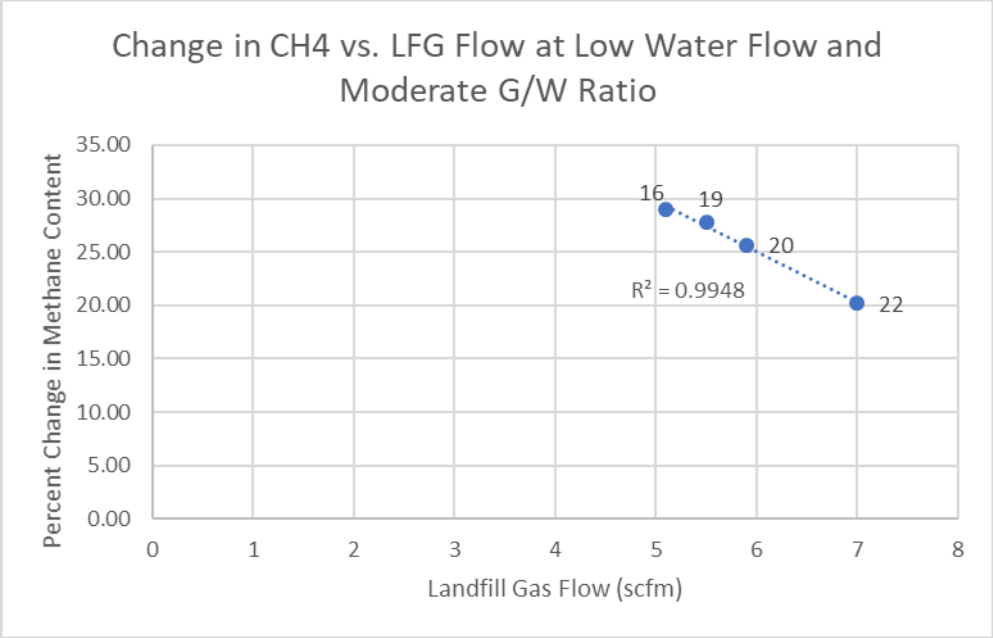

Fig. 22: The change in landfill gas methane content versus landfill gas flow rate at low water flow rates and moderate gas/water ratios—Data labels indicate water flow rate (gpm)

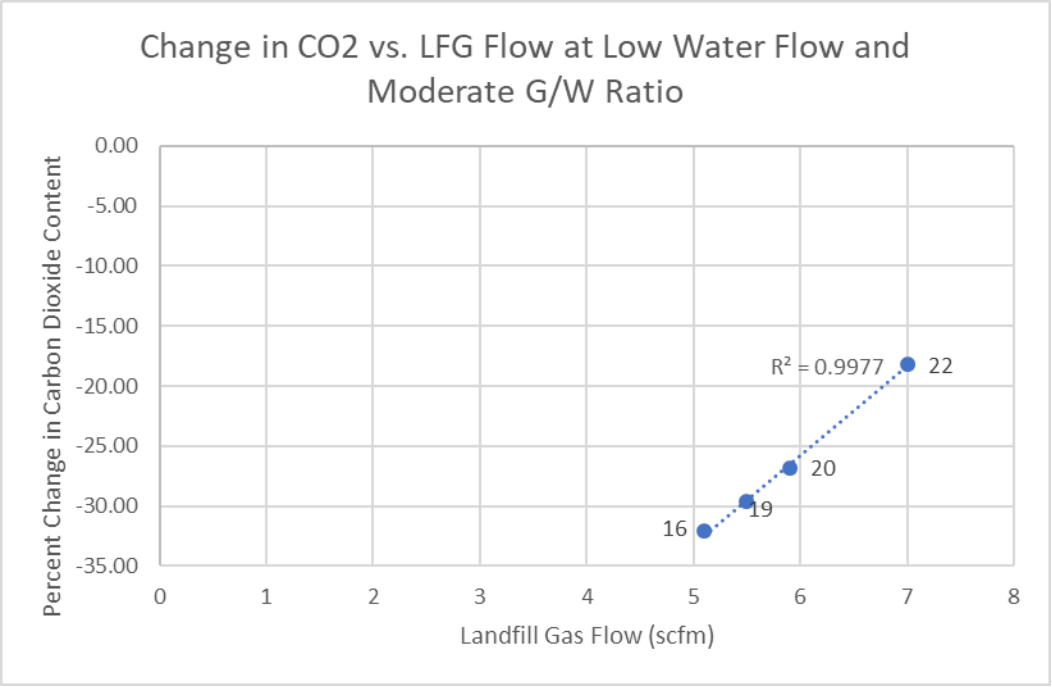

Fig. 23: The change in landfill gas carbon dioxide content versus landfill gas flow rate at low water flow rates and moderate gas/water ratios—Data labels indicate water flow rate (gpm)

Purity of product gas.

In this paper, the percent of landfill gas consisting of methane, oxygen, and nitrogen is referred to as percent methane equivalent. Percent methane equivalence was calculated by assuming that carbon dioxide and methane are the only elements present in the gas. Nitrogen and oxygen, the only two other elements that were measured in the landfill gas, are both inert in the water wash process, as neither dissolves easily in water like carbon dioxide. Because of this relationship, methane, oxygen and nitrogen in the gas are considered one unit in this paper—the components of the gas which are not removed in the water wash. Figures 24 and 25 are shown below and show how the percent methane equivalent of the product gas changes with water flow rate and landfill gas flow rate. They also include data labels listing the corresponding landfill gas and water flow rates, respectively, for each point.

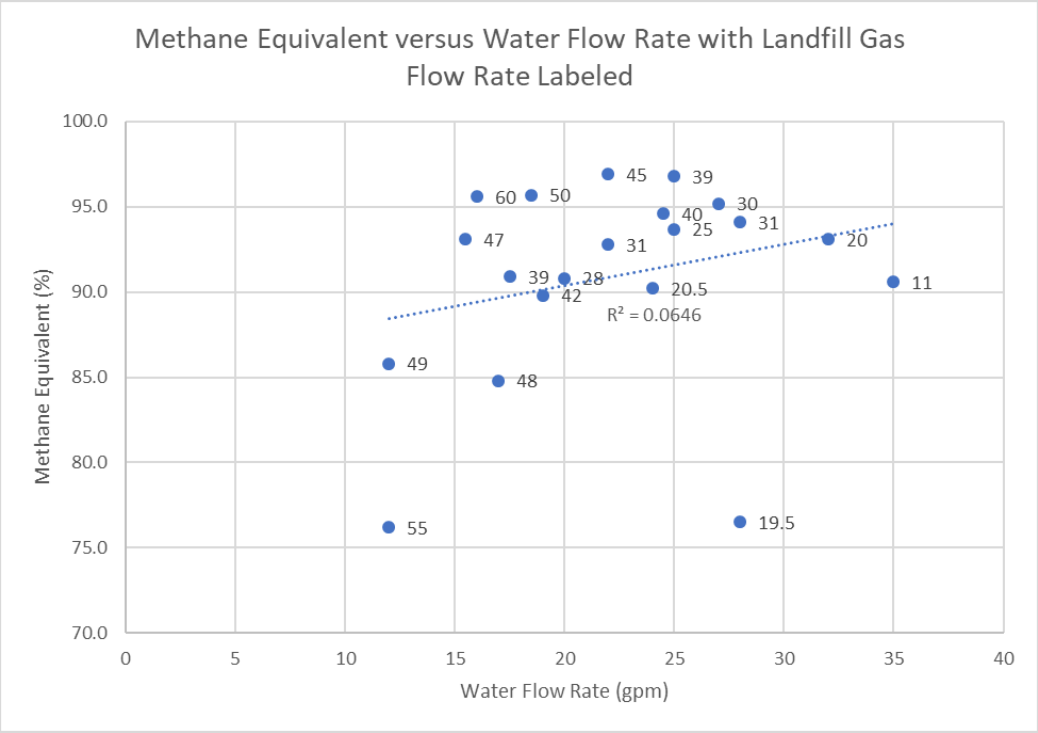

Fig. 24: Change in percent methane equivalent with variation in water flow rate—The data labels indicate landfill gas flow rate (scfm)

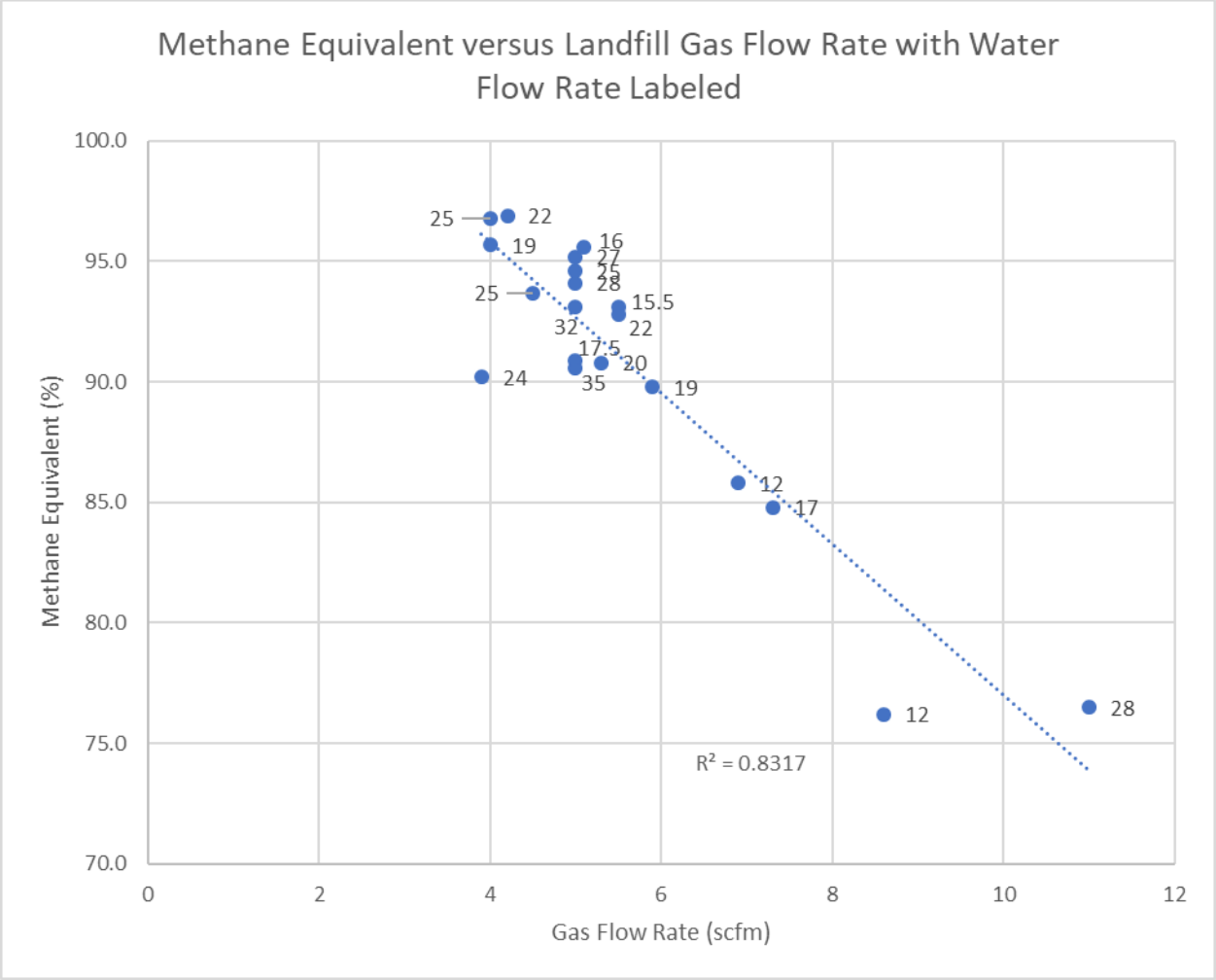

Fig. 25: Change in percent methane equivalent with variation in landfill gas flow rate—The data labels indicate water flow rates (gpm)

Energy consumption.

Based on the measured flows and pressures of the system process water and landfill gas, the power requirements necessary to pump the water and compress the gas were calculated given Equations 3 and 4 below (Engineering Toolbox, 2008):

Water Horsepower: $HP = Flow \times Pressure/1715$ Equation 3

Where: Flow is given in gallons per minute

Pressure is given in pounds per square inch

Single-Stage Gas Horsepower: $HP = \frac{144 \times P_1 \times V \times k}{33000 \times (k-1)} \times [(\frac{P_2}{P_1})^{\frac{k-1}{k}} - 1]$ Equation 4

Where: P_1 is initial absolute pressure (14.7 psi)

P_2 is final (compressed) absolute pressure in psi

V is the volumetric flow rate of the gas at atmospheric pressure at scfm

K is the adiabatic expansion coefficient (1.41)

Figures 26-28 below show the relationship between power consumption of the system and methane equivalence of the product gas. Figures 26 and 27 focus on the power consumed to compress the gas before it enters the absorbers and to pump the water through the system, respectively. Figure 28 shows methane equivalence versus total power consumed to compress and pump the gas and water.

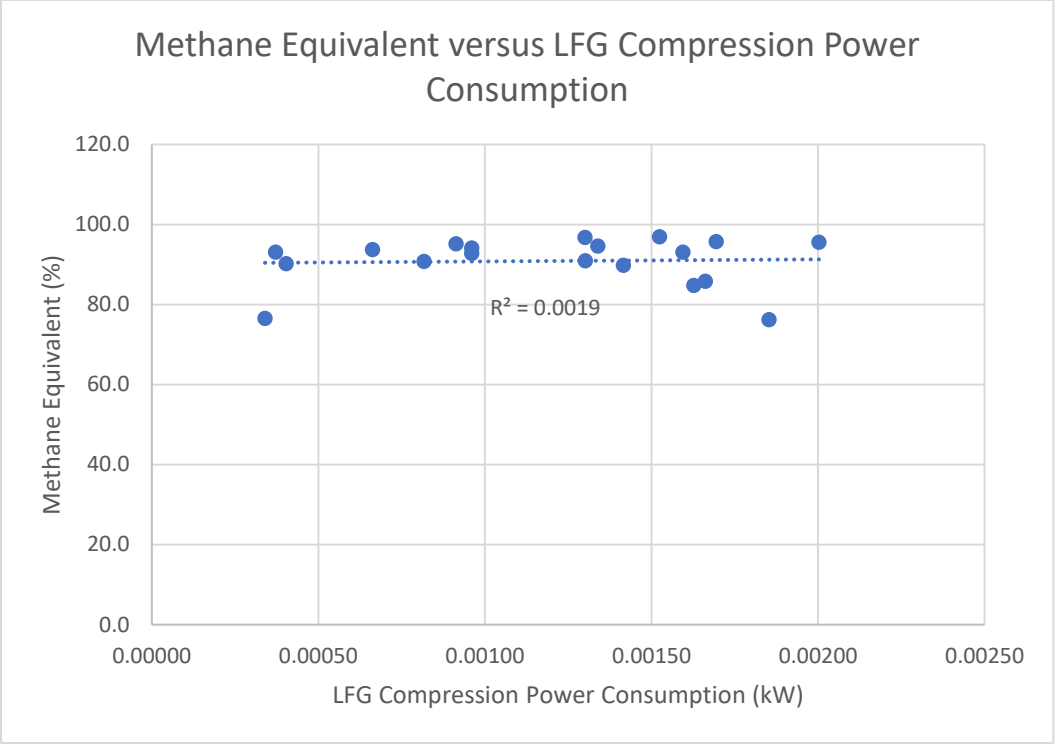

Fig. 26: Percent methane equivalent versus power consumed to compress landfill gas

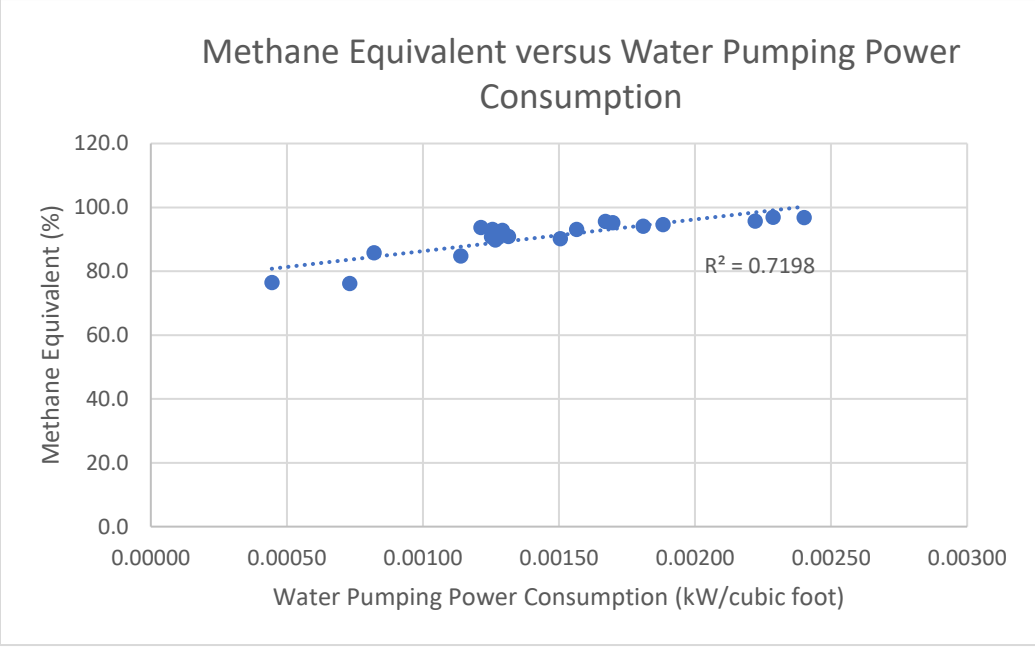

Fig. 27: Percent methane equivalent versus power consumed to pump water

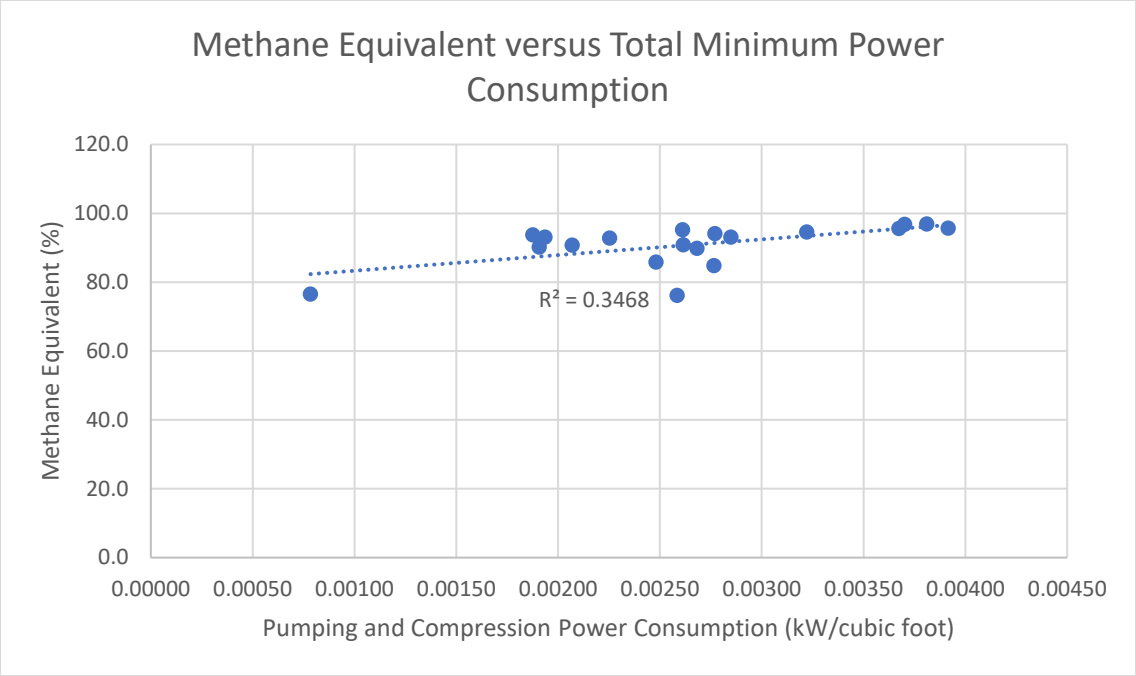

Fig. 28: Percent methane equivalent versus total power consumed to pump process water and compress gas

Chapter 4: Discussion

Water Wash Findings

From Figures 5-7, it appears that the gas flow rate is the independent variable with the greatest effect on system efficiency, with an R^2 value of 0.8064. Figure 5 shows a decline in performance index as landfill gas flow rate increases. This is as expected, because faster gas flow rates allow for less contact time between the gas and process water, so less carbon dioxide is absorbed. Gas/water ratio appears to only have a moderate negative correlation with performance index, while water flow rate shows no correlation at all. This is likely because water flow through the system was limited by low pressure from the water source. If more water pressure were available, runs with a greater range of water flow rates could have been measured. It is expected that future experiments with this system will

include a water source with higher pressure to alleviate this issue. Figures 8 and 9 show an excellent correlation between the change in landfill gas makeup and performance index, each with R^2 values of 0.93 and higher. The graphs both show the expected relationship between methane or carbon dioxide content and performance index based on Equations 3 and 4. A significant decrease in carbon dioxide content would indicate a similar significant increase in methane content, and a higher performance index value. It is important to note when evaluating Figures 5-15, however, that due to system settings, not all variables were controlled for each run. All three independent variables often changed from run to run, rather than only a single control variable. These pilot adjustments were made to prevent flooding of the absorption column. When a column becomes flooded, water flow inside the column becomes more stagnant, and gas mixing decreases. This is because bubbles form as the gas rises through the water-filled column, resulting in lower mixing efficiency between the gas and water. It is therefore important to operate the system like this to prevent flooding. If the gas flow is increased, for example, the pressure inside the column would also increase, causing an increase in water pressure to match the operational gas pressure. At the same time, the water flow was increased or decreased to achieve the desired gas:water ratio, and the system was monitored to prevent flooding. Therefore, all three variables were changed each run.

Effect of water and gas inflow velocities.

Figures 10 and 11 show no correlation between water flow and carbon dioxide absorption or change in methane concentration. It was expected that increased water flow would result in greater absorption of carbon dioxide and higher quality product gas. Belaissaoui et al. (2016) found that increasing the water velocity through the column increased the amount of carbon dioxide absorbed, as well as the efficiency of the process. Likewise, Sugiharto et al. (2015) used Wilson and Margules

thermodynamic models to demonstrate the same relationship. This is because by increasing the velocity of water, its concentration of dissolved carbon dioxide is decreased, leading to increased transfer from gaseous to aqueous state (Belaissaoui et al. 2016).

This unexpected lack of correlation could be due to not all variables being controlled when collecting the data shown in these figures. It may be that gas flow has a greater effect on the process efficiency, and therefore any changes in gas flow may have dominated the results and hidden the effect of varying water flow rate. It is also possible that the effects of changing water flow are only apparent at a wider range of flows than were measured here.

Figures 12 and 13 indicate that greater landfill gas flow rates result in less absorption of carbon dioxide and less increase in methane content between the raw gas and product gas. The relationship between change in carbon dioxide or methane content and gas/water ratio shown in Figures 14 and 15 is similar, although the correlation to gas/water ratio is rather poor, while landfill gas flow shows a more moderate correlation to change in gas content. The poor correlation between carbon dioxide absorption and gas/water ratio may again be a result of low water flow rates. Sugiharto et al. (2015) found that under their evaluated conditions, the ideal liquid/gas ratio is about 3.5, or about 0.3 when converted to gas/water ratio. Most gas/water ratios in this experiment fell in a range between 1 and 2.5, much higher as compared to Sugiharto et al. (2015). With greater water flow, the gas/water ratio can be decreased to approach 0.3. It was also shown that decreasing the gas/water ratio in Aspen Plus simulations resulted in greater CO_2 absorption efficiency and purity of product gas, as greater water flow makes conditions more favorable to carbon dioxide absorption (Cozma et al., 2014).

The decline in carbon dioxide absorption and final methane content with higher gas flow rates and gas/water ratio was expected for the same reasons described earlier when discussing the relationship between gas content and performance index. Gas moving at a higher flow rate has less

contact time with the process water, and therefore less time for the carbon dioxide in the gas to absorb into the water. Belaissaoui et al. (2016), however, found that increasing gas flow velocity showed negligible effect on total carbon dioxide absorption. At the same time, they also found that it significantly affected the efficiency of carbon dioxide removal, as the efficiency was greatest at slow gas velocities. At gas velocities of about 0.01m/s, carbon dioxide removal in Belaissaoui et al.'s (2016) study varied between about 7-30%, depending on the water velocity. Carbon dioxide removal in this pilot test ranged from 13-33%, which is comparable.

The performance of the water wash system appeared to improve over time, which can be explained by increasing operator familiarity with the system. Figure 29 shows the change in methane content versus water flow for the first several runs of the absorber system. As in Figure 10, which shows the same data for all runs, no correlation between gas content and water flow rate seems apparent.

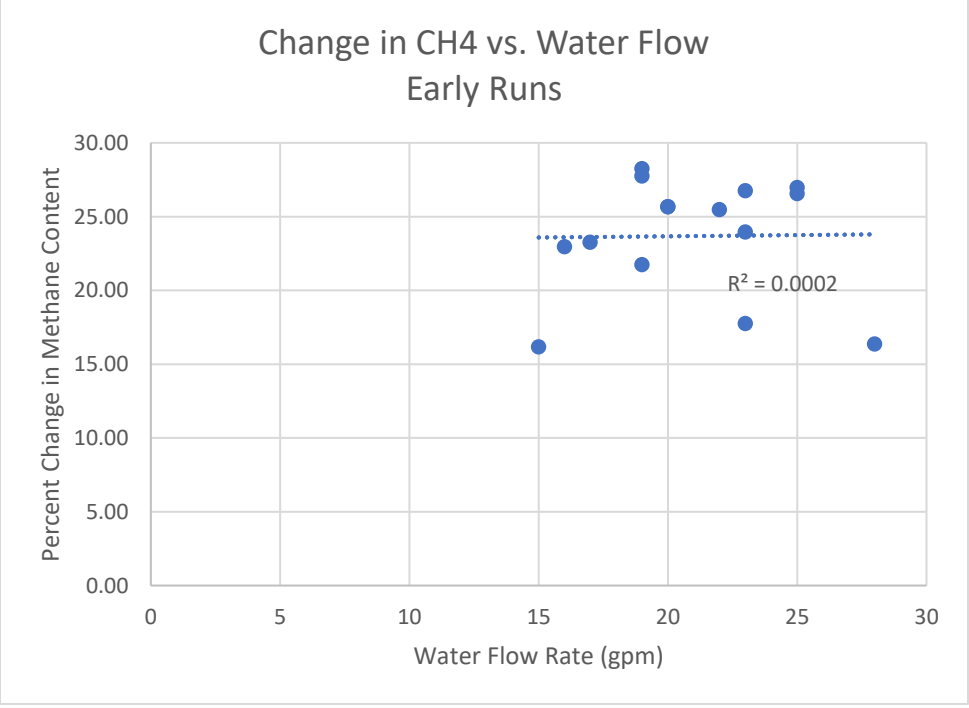

Fig. 29: Change in methane versus water flow rate for water wash system runs 11/30 to 12/11

Figure 30, on the other hand, shows the change in methane content of the landfill gas versus water flow rate for later runs, after system operation and performance had improved. The data collected later shows a relatively higher R^2 value than either Figure 10 or Figure 29, although it remains rather low. The figure also shows a possible correlation between water flow rate and performance. While the landfill gas pressure was not controlled for when collecting this data, Figure 30 does appear to show a general downwards trend in performance as the water flow rate increases. The data labels, which list the corresponding landfill gas flow rates for each data point, show a similar trend of improved performance with lower flow rates. Because the faster flow rate results in less contact time between the water and the gas, less carbon dioxide is absorbed, resulting in the declining performance with increased water flow. More experimentation is necessary to further evaluate the separate effects of varying water and gas flow rates on carbon dioxide absorption, apart from their combined influence.

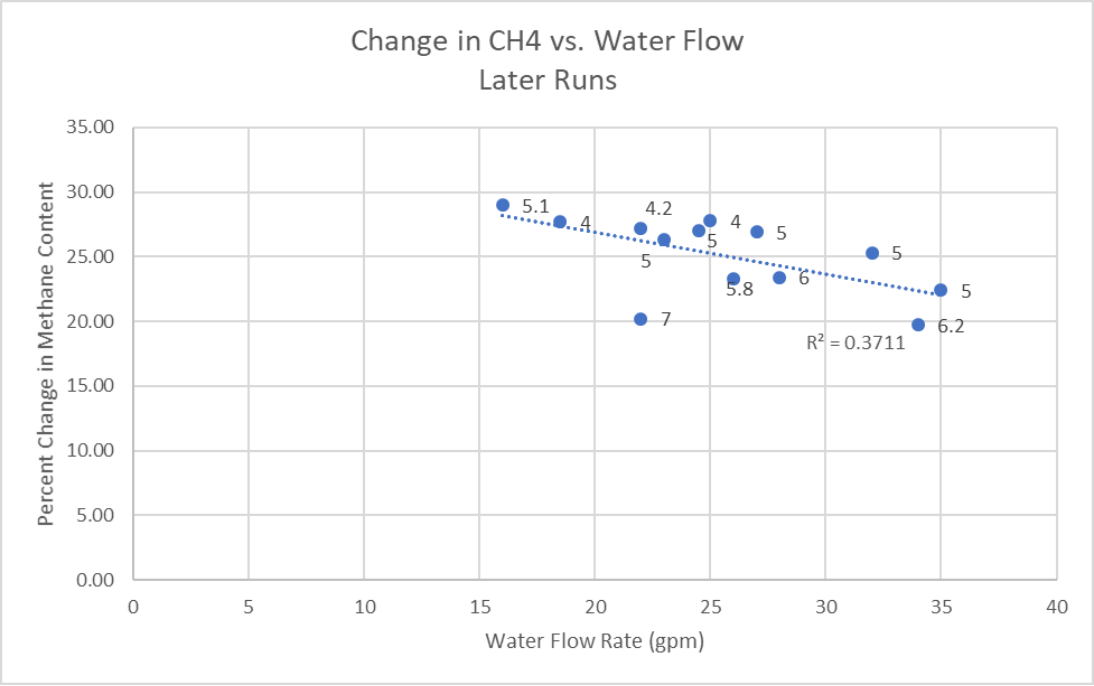

Fig. 30: Change in methane versus water flow rate for water wash system runs 12/12 to 12/19—The data labels indicate landfill gas flow rate (scfm)

Figures 31 and 32 similarly show the change in methane and carbon dioxide content, respectively, with change in landfill gas flow during the early system trials. As can be seen in Figures 33 and 34, the data from later runs fit the trendline better and continued to show a decrease in percent change of methane and carbon dioxide content with increasing gas flow rate. The later runs also show a clearer pattern between the data labels, which list water flow rate, and carbon dioxide absorption. Figures 33 and 34 show again that more carbon dioxide is removed from the landfill gas at lower flow rates for both gas and water. As in Figure 30, an increased flow rate decreases the amount of contact time between the water and gas streams in the absorption column, resulting in less time for the carbon dioxide to dissolve in the water stream.

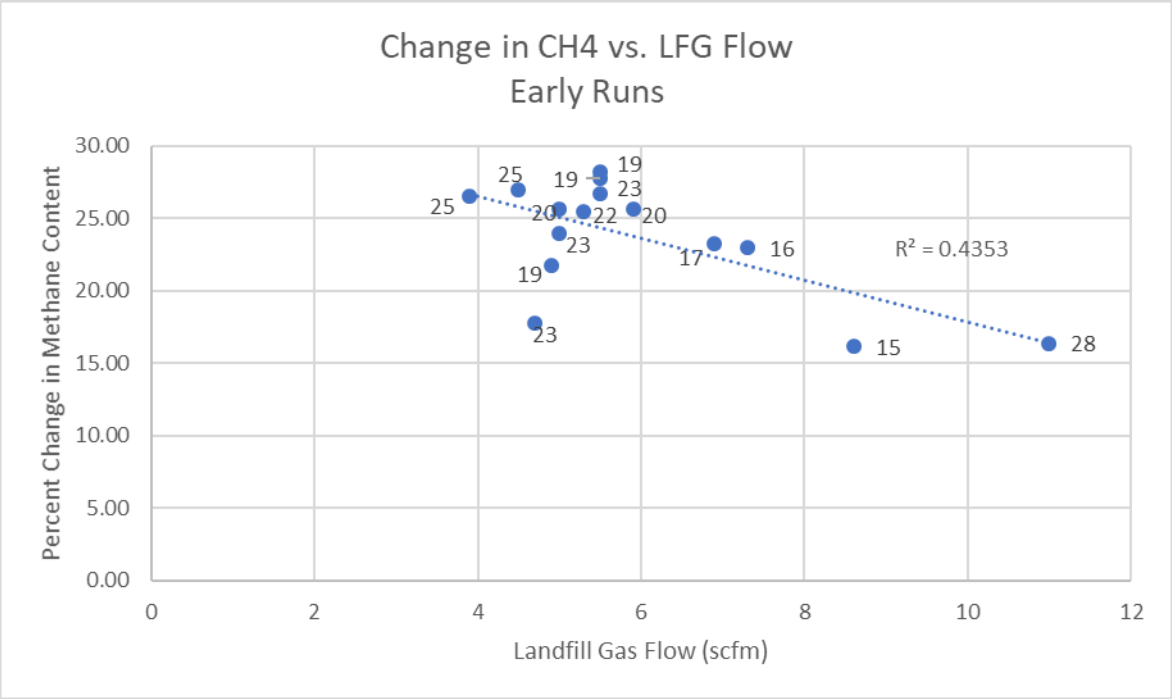

Fig. 31: Change in methane content versus landfill gas flow rate for water wash system runs 11/30 to 12/11—The data labels indicate water flows (gpm)

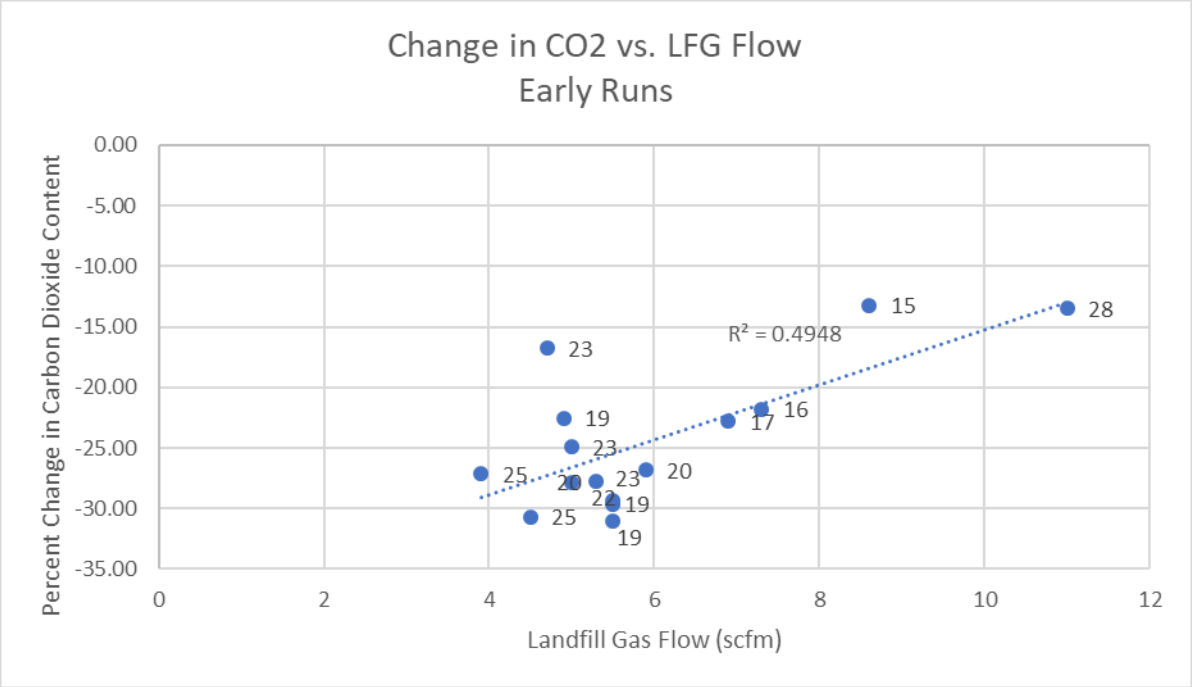

Fig. 32: Change in carbon dioxide content versus landfill gas flow rate for water wash system runs 11/30 to 12/11—The data labels indicate water flows (gpm)

-

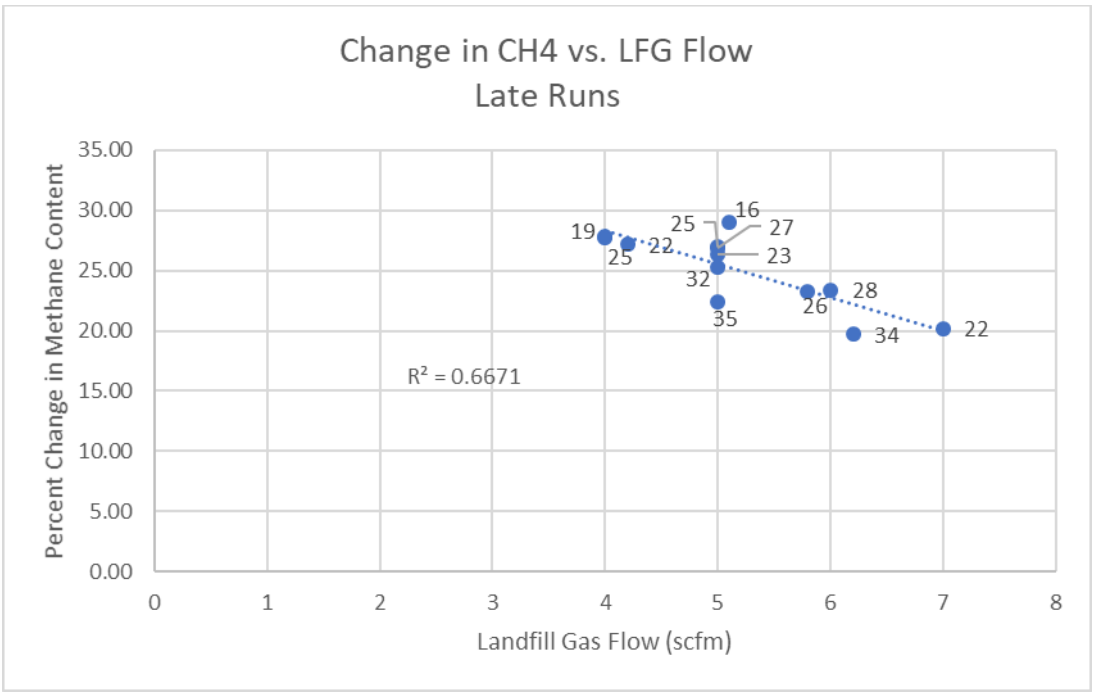

Fig. 33: Change in methane content versus landfill gas flow rate for water wash system runs 12/12 to 12/19—The data labels indicate water flows (gpm)

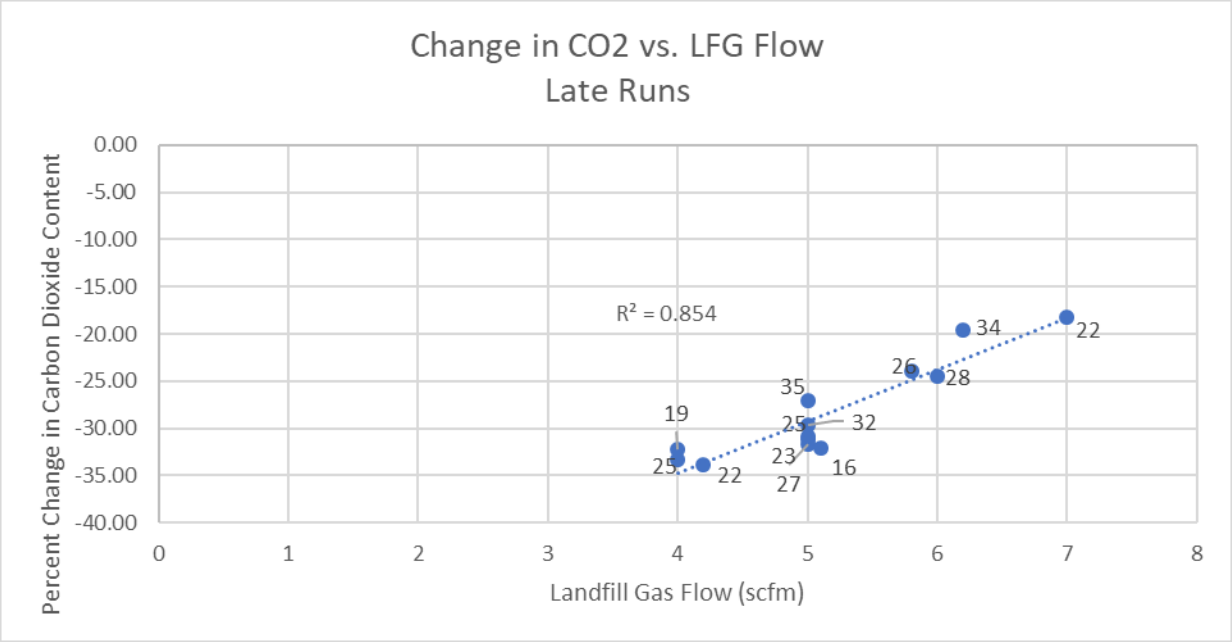

Fig. 34: Change in carbon dioxide content versus landfill gas flow rate for water wash system runs 12/12 to 12/19

Controlling for multiple variables.

The data labels in Figures 20 and 21 appear to indicate that in addition to increasing water flow, increasing landfill gas flow also affected the change in methane and carbon dioxide content. Figures 22 and 27 also appear to demonstrate the same relationship. These figures show decreased carbon dioxide absorption with increasing water and gas flows through the water wash column. It is likely that the changes in both water and gas flow shown in these figures both resulted in decreased absorption, rather than one variable alone. Increasing the flow of either stream would result in less contact time between water and gas, which is a significant factor affecting the amount of carbon dioxide absorbed into the water. More contact time results in greater absorption, while higher flows and the resulting higher velocities decrease this contact time.

As discussed in the results section, datapoints had to be grouped in such a way as to control for changing variables. Because the equilibrium of the absorber system had to be maintained when adjusting settings, both water and landfill gas flow rates had to be adjusted when setting up for a new run. Failure to adjust one flow rate to compensate for the other could result in either a flooded absorption column or a system with too little pressure to effectively dissolve carbon dioxide into the process water. Figures 5-15 do not account for the presence of multiple control variables in one dataset. While this issue was addressed in graphs such as Figures 20 and 21, which limit the range of the two control variables not being evaluated, it also presents the problem of limited datapoints. Figures 22 and 23, for example, each only have four plotted datapoints. The more limited a dataset is, the less statistically accurate it is likely to be. It is possible that dataset groupings with few datapoints do not reflect very well true averages and relationships between variables. Ideally, a continuation of this study would collect more data at or near these settings to supplement and support existing data.

Tables 5-7 describe the settings for each dataset grouping, including the control variable ranges, independent variable, and dependent variable. They also list the R^2 values for the associated graphs as a measure of correlation.

Change in Methane Content					
Gas/Water Ratio		**Water Flow**		**Landfill Gas Flow**	
Graph	**R Squared Value**	**Graph**	**R Squared Value**	**Graph**	**R Squared Value**
Low LFG Flow and Low-Moderate Water Flow	0.194	Low-Moderate LFG Flow and Low G/W Ratio	0.8178	Low Water Flow and Low G/W Ratio	0.5425
Moderate LFG Flow and High Water Flow	0.7797	Low-Moderate LFG Flow and Low-Moderate G/W Ratio	0.5312	Low Water Flow and Moderate-High G/W Ratio	0.9105
Low-Moderate LFG Flow and Low-Moderate Water Flow	0.7489	Moderate-High LFG Flow and Moderate G/W Ratio	0.1803	Low Water Flow and Moderate G/W Ratio	0.9948
Moderate-High LFG Flow and Moderate-High Water Flow	0.5289			High Water Flow and Low G/W Ratio	0.6371
High LFG Flow and Low Water Flow	0.3217				

Table 5: R^2 values for variable-controlled datasets with a dependent variable of change in methane content

Change in Carbon Dioxide Content					
Gas/Water Ratio		**Water Flow**		**Landfill Gas Flow**	
Graph	**R Squared Value**	**Graph**	**R Squared Value**	**Graph**	**R Squared Value**
Low LFG Flow and Low-Moderate Water Flow	0.2101	Low-Moderate LFG Flow and Low G/W Ratio	0.4114	Low Water Flow and Low G/W Ratio	0.6535
Moderate LFG Flow and High Water Flow	0.7649	Low-Moderate LFG Flow and Low-Moderate G/W Ratio	0.4429	Low Water Flow and Moderate -High G/W Ratio	0.9207
Low-Moderate LFG Flow and Low-Moderate Water Flow	0.2607	Moderate - High LFG Flow and Moderate G/W Ratio	0.1564	Low Water Flow and Moderate G/W Ratio	0.9977
Moderate-High LFG Flow and Moderate - High Water Flow	0.3715			High Water Flow and Low G/W Ratio	0.5634
High LFG Flow and Low Water Flow	0.3001				

Table 6: R^2 values for variable-controlled datasets with a dependent variable of change in carbon dioxide content

Performance Index					
Gas/Water Ratio		**Water Flow**		**Landfill Gas Flow**	
Graph	**R Squared Value**	**Graph**	**R Squared Value**	**Graph**	**R Squared Value**
Low LFG Flow and Low-Moderate Water Flow	0.2205	Low-Moderate LFG Flow and Low G/W Ratio	0.3516	Low Water Flow and Low G/W Ratio	0.7188
Moderate LFG Flow and High Water Flow	0.7616	Low-Moderate LFG Flow and Low-Moderate G/W Ratio	0.4394	Low Water Flow and Moderate -High G/W Ratio	0.9176
Low-Moderate LFG Flow and Low-Moderate Water Flow	0.2744	Moderate - High LFG Flow and Moderate G/W Ratio	0.1647	Low Water Flow and Moderate G/W Ratio	0.9945
Moderate - High LFG Flow and Moderate - High Water Flow	0.36			High Water Flow and Low G/W Ratio	0.5417
High LFG Flow and Low Water Flow	0.3251				

Table 7: R^2 values for variable-controlled datasets with a dependent variable of performance index

It is clear from Tables 5-7 that, as in the initial data analysis of the entire dataset as a whole, landfill gas flow rate had the greatest predictable effect on performance of the water wash system in this experiment. The R^2 values for graphs evaluating landfill gas flow are consistently higher than those evaluating water flow and gas/water ratio, indicating that the data is a better fit to the gas flow regression lines. Correlation of landfill gas flow rate to performance index and change in methane and carbon dioxide is moderate to good, while the correlations between the dependent variables and gas/water ratio or water flow rate are generally moderate to poor, with few exceptions, such as the change in methane content versus water flow rate at low-moderate landfill gas flow and low gas/water ratios (shown in Figure 24).

Comparison to modeled results.

Prior to installation of the water wash pilot project, Bashar (2018) used Aspen Plus Simulation software to model the planned system. This model predicted 98% methane content in the product gas at 60 degrees Fahrenheit and 45psi. The calculated product gas methane equivalent results from this experiment reached as high as 96.7%, with the majority of runs producing methane equivalent results of greater than 90%. The average methane equivalent in the product gas for all viable runs was 90.9%. This is lower than the modelled results because the low water pressure prevented the system from being run with two absorbers. With greater water pressure, higher carbon dioxide removal would be expected, along with greater percent methane equivalent values. Additionally, the water dispersion in the system as well as the packing material may also have played a role in differences between the model and the pilot test results, as the actual dispersion material may have been different from that modeled. When only one absorber was modeled in the Aspen Plus software, product gas methane contents of about 92-96% were predicted. It predicted a maximum methane content of 97.9% with one absorber

and process water at a temperature of 40 degrees Fahrenheit. Process water in the pilot system was typically about 50 degrees. While the system has no way of controlling for water temperature, it is located outdoors, and seasonal fluctuations in temperature are expected. Because of the decreased solubility of carbon dioxide in water at higher temperatures, the system is expected to be more efficient during cold weather.

Energy consumption findings.

Figure 37 shows the power consumption for pumping and compressing the process water and air for early runs of the system, and Figure 38 shows the same data for later runs.

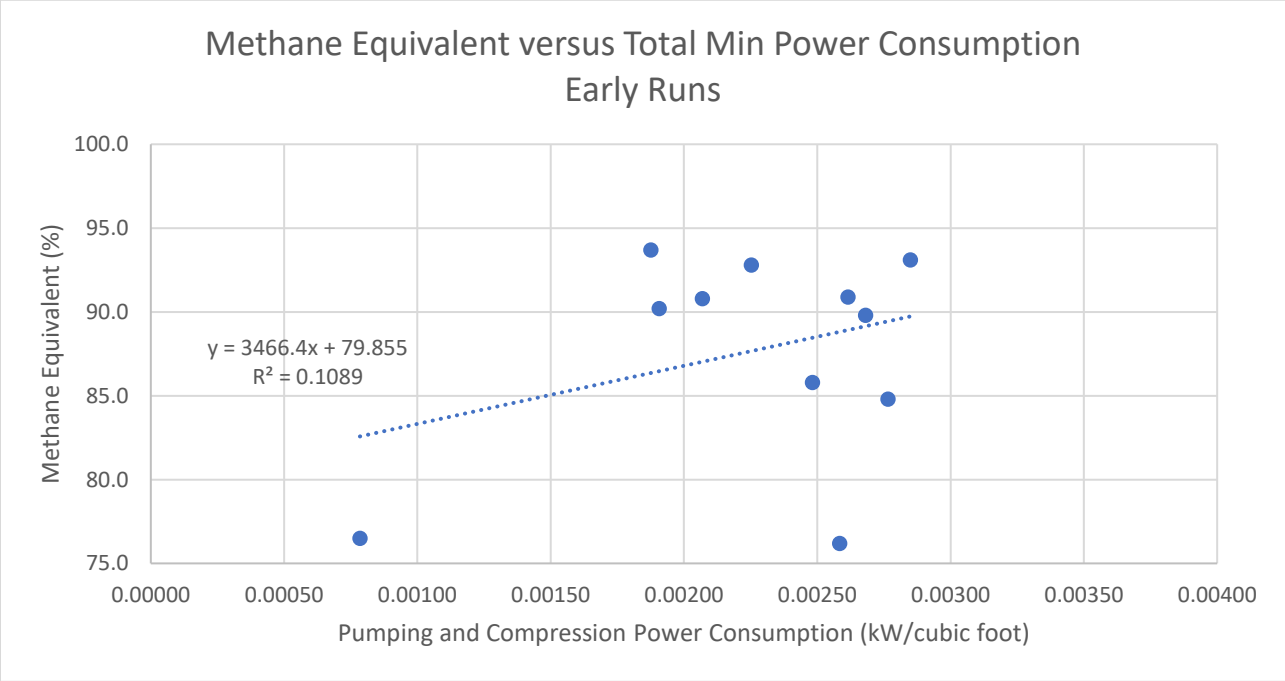

Fig. 35: Methane equivalent versus total minimum power consumption for runs dated 11/30/18 to 12/11/18

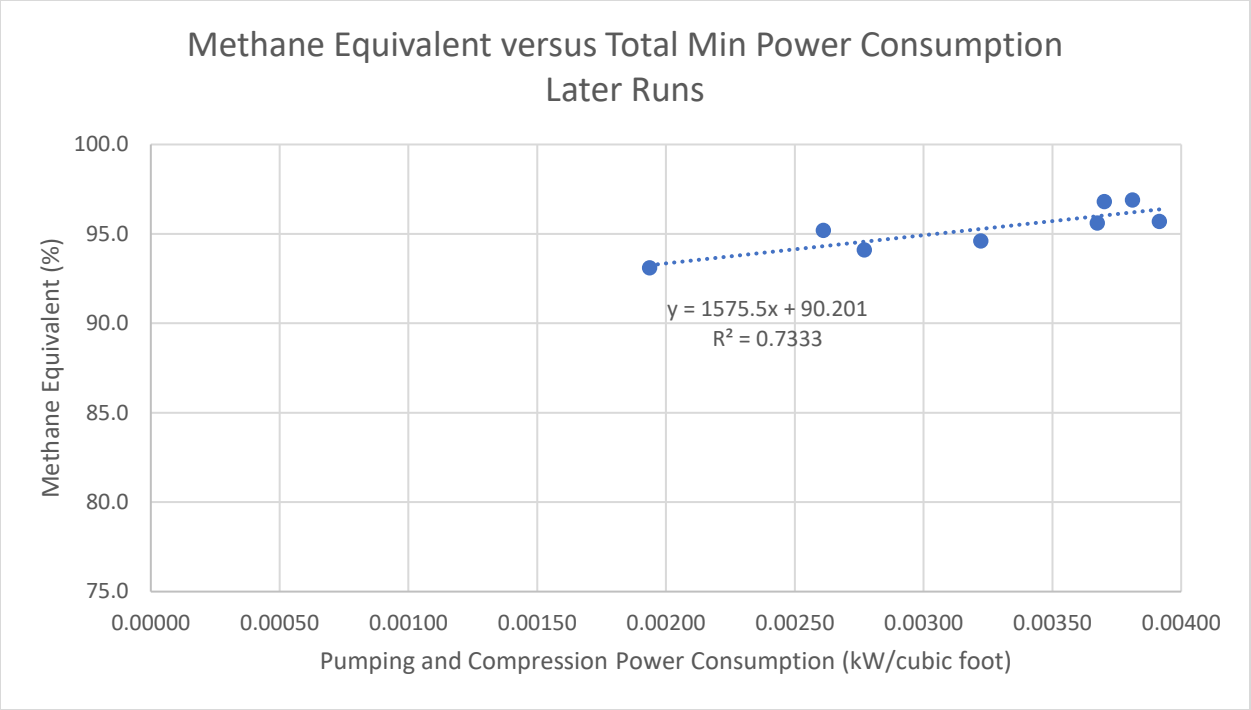

Fig. 36: Methane equivalent versus total minimum power consumption for runs dated 12/12/18 to 12/19/18

Both Figures 37 and 38 show a general upwards trend of methane equivalent with power consumption. It is clear that the results of the later runs were more consistent, with a much better fit of the data points to the trendline—The R^2 value of Figure 38 is much higher than that of Figure 37, making the positive relationship between power consumption and percent methane equivalent clearer.

Nock et al. (2014) reported energy usage of 0.23kWh/Nm^3, or 0.00652kWh/scf at 10 bar. Energy consumption calculated in this experiment are much lower, with most falling within a range of 0.002-0.004kWh/scf. Nock's value is more than 50% greater than the highest energy usage datapoint shown in Figure 27. Studies referenced by Nock show even greater anticipated energy requirements. Cozma et al. (2013), meanwhile, report energy consumption of 0.016kWh/scf.

Chapter 5: Conclusions

Landfill gas flow rate had the strongest effect on performance index and increase in methane content/decrease in carbon dioxide content of the gas. More carbon dioxide was removed a low flow rates, and around 4-6 scfm, 20-35% decreases in carbon dioxide were measured. Little correlation was found to water flow rate, most likely due to only low water flow rates being used in this experiment. Likewise, the correlation of system performance to gas/water ratio was only moderate. A greater range of water flow rates would have provided more opportunity to study this relationship. The results of the water wash experiment matched those predicted by the Aspen Plus modeling software. The software predicted methane content of 92-96% in the product gas, depending on water flow, and this experiment measured similar methane equivalent values.

Future experiments with this pilot system will include a greater range of water flow rates, as more pressure will be provided to the system. This will not only allow better evaluation of the relationship between water flow, gas/water ratio, and product gas purity, but it will also allow the system to be operated utilizing both absorbers, and the flash columns, rather than one single absorber. This will also allow the effect of packing material size to be examined, as well as that of series versus parallel configuration of the absorbers.

References

Bashar, M. A. (2018). *Biogas quality improvement using water wash and phosphorus recovery as struvite in Jones Island WWTP* (Unpublished master's thesis). University of Wisconsin-Milwaukee, Milwaukee, United States.

Belaissaoui, B., Claveria-Baro, J., Lorenzo-Hernando, A., Zaidiza, D. A., Chabanon, E., Castel, C., Sabine, R., Roizard, D., & Favre, E. (2016). Potentialities of a dense skin hollow fiber membrane contactor for biogas purification by pressurized water absorption. *Journal of Membrane Science, 513,* 236-249.

Bortoluzzi, G., Gatti, M., Sogni, A., & Consonni, S. (2014). Biomethane production from agricultural resources in the Italian scenario: Techno-economic analysis of water wash. *Chemical Engineering Transactions, 37*, 259-264. DOI: 10.3303/CET1437044

Carbon Dioxide. (2018). Retrieved April 22, 2019, from https://webbook.nist.gov/cgi/cbook.cgi?ID=C124389&Mask=10#Solubility

Cozma, P., Ghinea, C., Mămăligă, I., Wukovits, W., Friedl, A., & Gavrilescu, M. (2013). Enviromental impact assessment of high pressure water scrubbing biogas upgrading technology. *CLEAN—Soil, Air, Water, 41*(9), 917-927. DOI 10.1002/den201200303

Cozma, P., Wukovits, W., Mămăligă, I., Friedl, A., & Gavrilescu, M. (2014). Modeling and simulation of high pressure water scrubbing technology applied for biogas upgrading. *Clean Technologies and Environmental Policy, 17*(2), 373-391. DOI 10.1007/s10098-014-0787-7

Dodds, W. S., Stutzman, L. F., & Sollami, B. J. (1956). Carbon dioxide solubility in water. *Industrial and Engineering Chemistry, 1*(1), 92-95.

Energy Tech Innovations, LLC. (2016). *Supplemental information/ETI reference data 11/7/2016* (Informational brochure).

Engineering ToolBox, (2008). Horsepower required to compress air: Online air compressor horsepower calculator [online]. Retrieved from: https://www.engineeringtoolbox.com/horsepower-compressed-air-d_1363.html

Hydrogen Sulfide. (2018). Retrieved April 22, 2019, from https://webbook.nist.gov/cgi/cbook.cgi?ID=C7783064&Units=SI&Mask=10#Solubility

Methane. (2018). Retrieved April 22, 2019, from https://webbook.nist.gov/cgi/cbook.cgi?ID=C74828&Units=SI&Mask=10#Solubility

Nock, J. W., Walker, M., Kapoor, & R., Heaven, S. (2014). Modeling the water scrubbing process and energy requirements for CO_2 capture to upgrade biogas to biomethane. *Industrial & Engineering Chemistry Research, 53*(32), 12783-12792. DOI 10.1021/ie501280p

Rasi, S. (2009). *Biogas composition and upgrading to biomethane* (Doctoral dissertation). University of Jyväskylä, Finland.

Sugiharto, A., Sutijan, S., & Hidayat, M. (2015). Sensitivity analysis of water scrubbing process for biogas purification, presented at The 2nd International Conference on Engineering Technology and Industrial Application, Surakarta, 2015. DOI: 10.13140/RG.2.1.3142.9206

Tynell, Å., Börjesson, G., & Persson, M., (2007). Microbial growth on pall rings. *Applied Biochemistry and Biotechnology, 141*, 299-319.